STRATIGRAPHIC STUDY AND JOINT-PATTERN ANALYSIS IN THE BIWABIK IRON FORMATION, VIRGINIA HORN AREA, NORTHEAST MINNESOTA

A THESIS
SUBMITTED TO THE FACULTY OF THE GRADUATE SCHOOL
OF THE UNIVERSITY OF MINNESOTA
BY

Kimberly Jane Neilson

IN PARTIAL FULFILLMENT OF THE REQUIREMENTS
FOR THE DEGREE OF
MASTER OF SCIENCE

September, 2003

ABSTRACT

The Biwabik Iron Formation of the Mesabi Range in northeastern Minnesota is comprised of chemically precipitated minerals. Cherty (granular) iron-formation formed on a shallow, tidally-influenced shelf, while slaty (fine-grained) iron-formation formed in deeper water.

Thirty-nine sections from a 311-foot long drill core taken from north of the EVTAC pit area were studied to determine the mineralogy and paragenesis of the formation. Growth textures and crosscutting relationships indicate the primary minerals are chert (cement), greenalite, hematite and siderite. Very fine-grained carbonaceous material was deposited simultaneously. Secondary minerals include ankerite, magnetite, minnesotaite, and stilpnomelane. There were multiple generations of chert, minnesotaite, and siderite. Minnesotaite and magnetite replaced chert, iron-silicates, and iron-carbonates. Ankerite replaced chert and iron-silicate and grew in close association with magnetite. Magnetite was not replaced by any mineral, and grew abundantly in the cherty iron formation. Stilpnomelane grew abundantly in the slaty iron-formation.

A study of joint orientations was undertaken on the premise that the data would be of value in planning the orientations of blasting grids at taconite pits. There are common joint orientations in seven taconite pits near the Virginia Horn area. The joints do not appear to vary with the strike of the iron-formation in the anticline/syncline structure of the Virginia Horn, and dips are generally vertical. A dominant joint direction found in Archean rocks of the Virginia Horn area (280°) is close to the dominant fault strike direction (285°) in the Virginia Horn, suggesting some control of the iron-formation jointing by underlying Archean basement rocks.

TABLE OF CONTENTS

Page

LIST OF FIGURES

LIST OF TABLES

ACKNOWLEDGEMENTS

Many thanks to Dr. Richard Ojakangas, Dr. Penelope Morton, Dr. James Grant, Dr. Timothy Holst, Dr. Thomas Johnson, Peter Jongewaard, Robert Waidler, John Arola, Steve Mekkes, Frank Pezzutto, Dana Scubik, Mark Jirsa, Terry Boerboom, the faculty, staff, and students at UMD, my family, my friends, and my coworkers for your support, knowledge, patience, and assistance.

Introduction:

Iron-formations are unique, iron-rich rocks of Precambrian age, which are located around the world in nearly all of the shield areas (Gross, 1973). Precambrian iron-formations are a separate entity from younger ironstones. Iron-formation is defined as "a chemically precipitated sedimentary rock that contains appreciable silica and typically more than 15% iron" (James, 1954). The definition was created in reference to the iron-rich rocks of the Lake Superior Region but the term has been used for discoveries of similar iron-rich sedimentary rocks of Precambrian age across the world.

Taconite is the common term used for the magnetite-rich iron-formation of the Lake Superior region (Figure 1). Early Proterozoic age iron-formations host most of the world's iron ore (Simonson, 1987), and 90% of the iron extracted globally has come from them (Isley, 1995). The Biwabik Iron Formation of the Lake Superior region has been a major source of the world's supply of iron since 1892 (Boese, 1975, p. 2).

In Minnesota there are three distinct geographic areas, or ranges, of exposed iron-formation, referred to as the Mesabi, Cuyuna and Gunflint (Figure 1). The Mesabi Range is the largest source of iron ore in the United States and the iron-formation is known as the Biwabik Iron Formation. Over 525 mines have removed ore from the Mesabi Range in the last century (Morey, 1999).

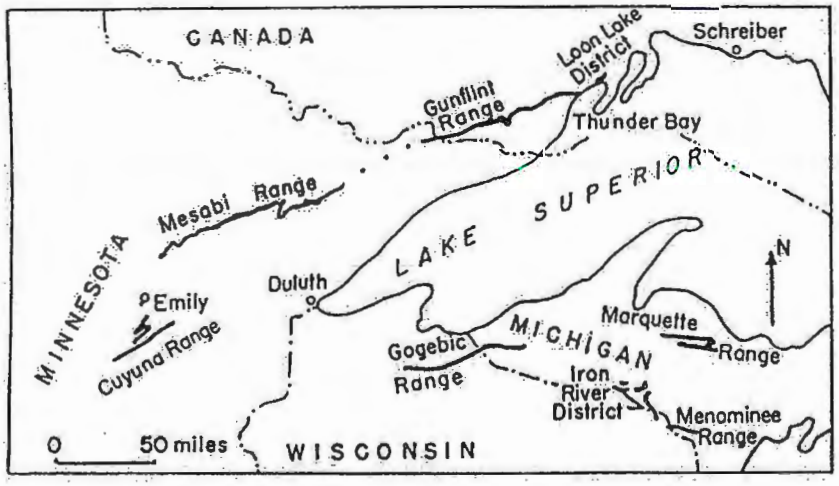

Figure 1. Iron ranges in the Lake Superior Region. From White, 1954, p. 2.

Location:

The Biwabik Iron Formation of the Mesabi Range forms a ribbon of outcrop in northern Minnesota. It extends from Grand Rapids in the west to beyond Babbit in the east (Figure 2), varies from 0.4 to 5 km wide, and extends for 200 km along a roughly northeast/southwest strike. It varies in thickness from less than 30 m to near 230 m (Morey, 1999). The dip is about 10° to the southeast. The structure of the Biwabik Iron Formation has a major bend, the "Virginia horn", consisting of a southwestward-plunging syncline and a parallel anticline near the city of Virginia, Minnesota. Due to glacial cover, the extent of the Biwabik Iron Formation is poorly defined west of Grand Rapids. At its eastern end, it is intruded by Middle Proterozoic gabbro of the Duluth Complex.

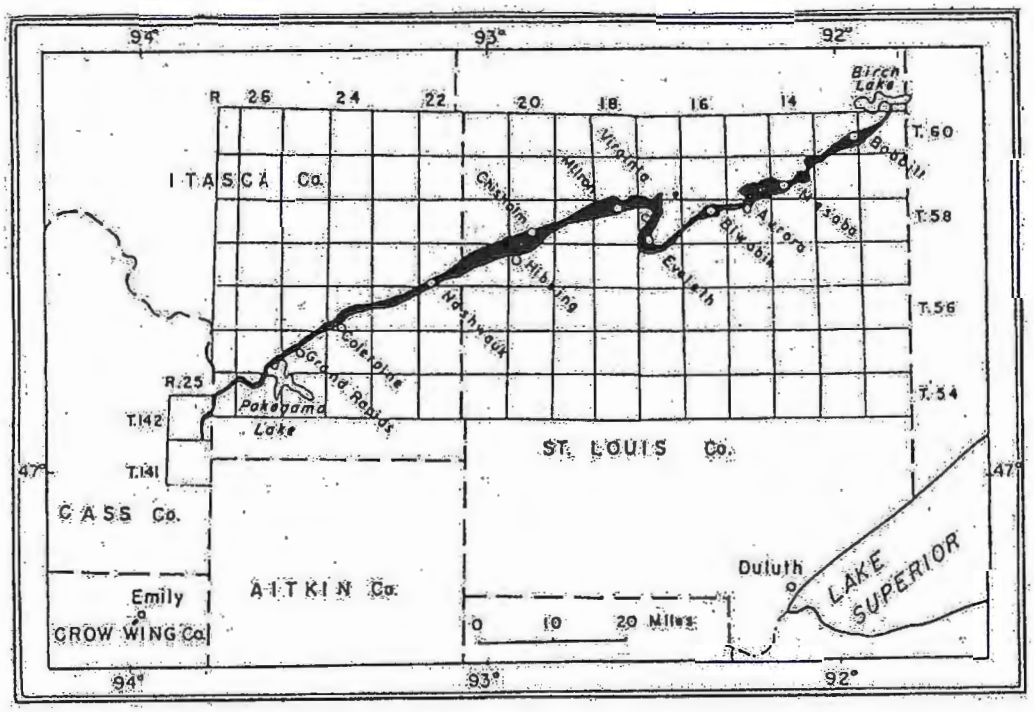

Figure 2. Mesabi Range, Minnesota. From White, 1954, p. 2.

Statement of Problem:

Debate and speculation surround theories regarding the origin of Precambrian iron-formation. There are no modern analogs of siliceous iron-formation, so attempts to elucidate the environment of deposition, the source of the iron and silica, the original iron minerals, and the conditions of the Precambrian atmosphere may never provide certain

answers (James, 1966). Research into these matters is important, though, because increased knowledge about iron-formation will allow more efficient mine placement and development, benefiting both mines and the environment (Gruner, 1946, p. 5).

Taconite is removed from the ground after it is blasted into manageable chunks with explosives (Clark, 1987, p. 4). Generally speaking, the amount of explosives used and the spacing and timing of the explosives controls the force of the blast and the size of the taconite pieces. The Biwabik Iron Formation contains pre-existing fractures, and it is useful to know the orientation of fractures for blasting purposes. Energy from the blast may be dissipated through the fractures, resulting in larger chunks (Figure 3) and less efficient use of materials, which creates the need for more processing of the taconite (Jongewaard, 1998).

Figure 3. Large pieces of blasted ore in an iron mine in northeastern Minnesota. Pencil provided for scale in middle-left foreground.

The purpose of this thesis is to provide data that may narrow down the answers to questions of the environment of deposition, the source of the iron and silica, the original minerals, and the conditions of the Precambrian atmosphere. In addition, an attempt was made to determine whether there is a discernable fracture pattern in the iron-formation in the vicinity of the Virginia horn.

Part I. Stratigraphic Study

Regional Geology:

Archean:

The Archean rocks in northern Minnesota are part of the Canadian Shield and consist of metamorphosed volcanic, volcano-sedimentary, and granitic rocks. Underwater volcanic centers, evidenced by pillow basalt, produced a mafic platform upon which felsic volcanic edifices were built. Erosion of these volcanic rocks, especially the felsics, produced sediments including graywackes deposited by turbidity currents (R. Ojakangas, 1972).

Folding and metamorphism of the Canadian Shield occurred during the 2.7 Ga Algoman orogeny, and the rocks are now oriented vertically in curvilinear belts. Granite batholiths intruded the volcanic-sedimentary piles, and regional metamorphism of the volcanic and volcano-sedimentary rocks created greenstone grade minerals. The resulting rocks are known as greenstone belts.

Animikie Basin:

The Animikie basin of the Early Proterozoic is interpreted as a northward-migrating foreland basin that developed in front of the fold-and-thrust belt formed by the Penokean orogeny (Hoffman, 1987; Southwick and Morey, 1991; R. Ojakangas, 1994; Morey, 1999). The Mesabi Range is found along the cratonic, or northern edge of the Penokean orogen. The orogeny occurred about 1.85 Ga due to the collision of island arcs and microcontinents with the southern margin of the Superior Province, giving rise to deformation, metamorphism, and plutonism. The uplifted rocks were a major source of sediment for the basin, and other sediment was derived from the Archean rocks to the north. However, there is a lack of terrigenous clastic detritus in the iron-formation. A package of siliciclastic rocks beneath the iron-formation, the iron-formation, and a thick overlying turbidite sequence comprise the Animikie Group of the Animikie basin, covering parts of Minnesota, Ontario, Wisconsin, and the Upper Peninsula of Michigan. Figures 4 and 5 show the location of the Mesabi Range with respect to the rocks and structural features in the Animikie Basin.

A U-Pb date of 1878.3 +/- 1.3 Ma has been obtained for the Gunflint Iron Formation (Fralick et. al, 2002). Morey (1970, p. 200) indicates that there is little doubt the Gunflint Iron Formation was continuous with the Biwabik Iron Formation before intrusion of the Duluth Complex.

Around 1.1 Ga, a mantle plume caused rifting and volcanism and created the Midcontinent Rift System and the Lake Superior syncline. The Mesabi Range is on the north limb of the syncline, dipping gently to the southeast. At least part of the dip of the iron-formation is due to the rifting event.

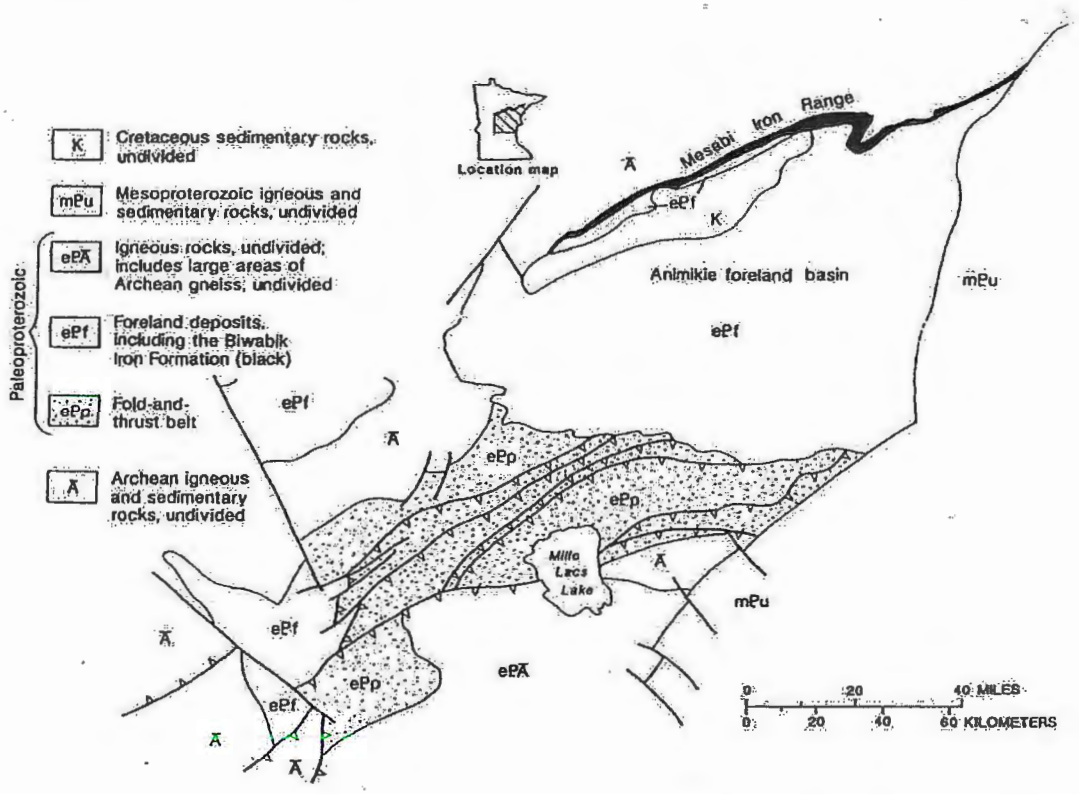

Figure 4. Geologic map showing the location of the Mesabi range with respect to the geologic features of the Animikie basin. Figure from Morey, 1999.

Biwabik Iron Formation:

The Biwabik Iron Formation is a banded iron-formation with a predominant mineralogy of chert, magnetite, hematite, iron silicates, and carbonates. Many scientists,

including Spurr, Leith, Gruner, Richarz, and Joliffe have worked to define and refine the mineralogical classifications (Gruner, 1946, p. 7). In the late nineteenth century, Spurr made a detailed description of the mineralogy of the central and western Mesabi Range. He considered the granular green minerals as one, and called them glauconite. At the turn of the century, Leith discovered that the green mineral was not glauconite, and called it greenalite. Due to what he called the "amorphous character" of the mineral, Leith did not further characterize the mineral. The mineral was generally thought to be an iron amphibole. About twenty years later, Richarz discovered that the "amphibole" did not exhibit the inclined extinction one would expect from monoclinic amphiboles. He considered the mineral to be mica and called it "crystallized greenalite." In 1934, while trying to assign a new formula to greenalite, Jolliffe simply described the amphibole-like mineral as "mineral X" and was unable to classify it. Using x-rays in 1944, Gruner was able to identify the three silicates making up the granular green mineral: minnesotaite, greenalite, and stilpnomelane.

Two main textural classifications, cherty and slaty, are recognized in the Biwabik Iron Formation (Spurr, 1894, p. 30). These terms are not meant to imply genesis of the rocks, but they describe the textural characteristics of the rock and the manner in which the iron-formation breaks. Cherty iron-formation is granular, massive, and rich in quartz and iron oxides. It breaks into chunks or slabs. Wavy bedding and cross bedding are the main depositional structures observed in outcrop of cherty iron-formation (Ojakangas, 1983). Both cherty and slaty iron-formation may be even or wavy bedded. Slaty iron-formation is composed of iron silicates and iron carbonates, and is fine-grained and finely laminated (Morey, 1970, p. 195). It tends to break into thin plates parallel to bedding, but it does not have a slaty cleavage produced by metamorphism. Beds of cherty and slaty iron-formation are interlayered on all scales, but the Biwabik Iron Formation has been roughly divided into four lithostratigraphic members: Lower Cherty, Lower Slaty, Upper Cherty, and Upper Slaty (Wolff, 1917; Gruner, 1946; White, 1954). These are further subdivided, usually into unique but compatible units, by the various mines along the range. In addition, researchers have adopted names for various sections of the iron-

formation based on quality of the ore, which is dictated by the character and distribution of the magnetite.

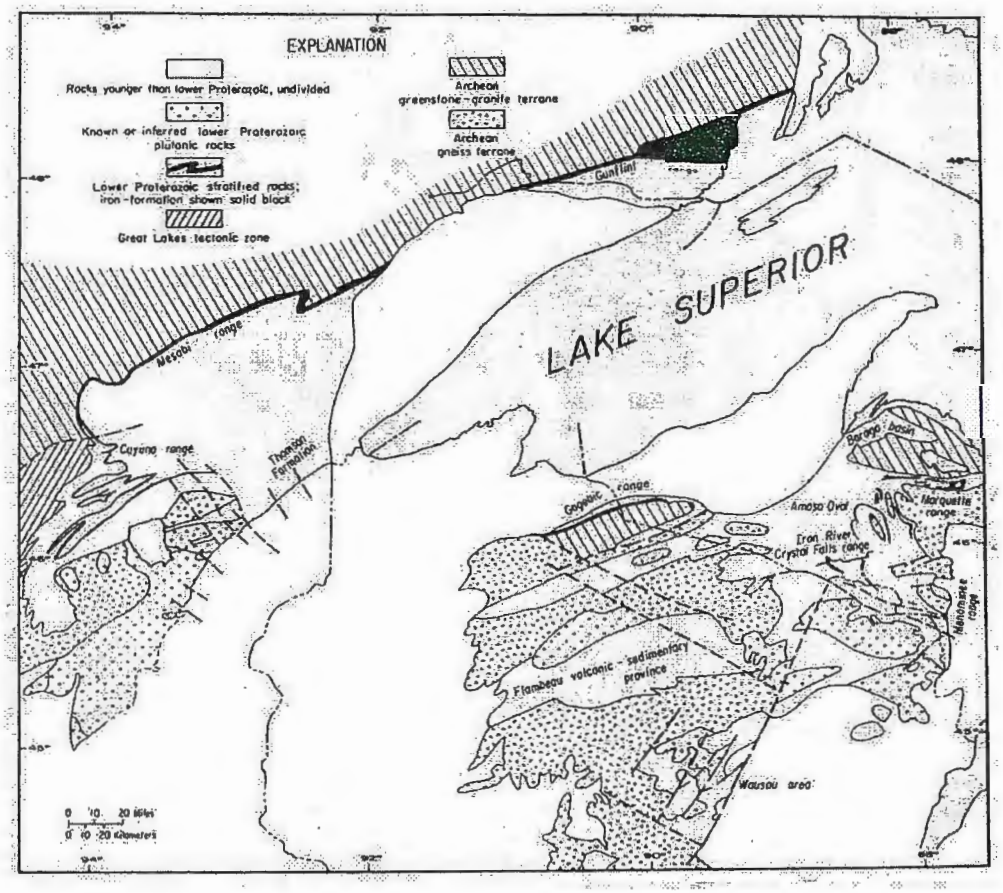

Figure 5. Geologic map showing the position of the Mesabi Range relative to other major components of the Penokean orogen in the Lake Superior region. From Morey, 1983.

Minerals in the cherty iron-formation and parts of the slaty iron-formation may be concentrated into granules. These granules, which average 0.5 mm in diameter, are what give the cherty iron-formation its coarser-grained appearance in hand specimen. Most granules have no internal structure and do not appear to be oolites, although some oolites have been found in the cherty iron-formation (White, 1954, p. 10).

Magnetite may be disseminated as octahedra or aggregates of crystals in regular or irregular bands, laminations, or mottled concentrations. These modifiers may be added to the rock name, taconite, to further describe the rock. For example, mottled cherty taconite would describe cherty-textured taconite with blebs of magnetite creating a

mottled pattern in the rock (Figure 6). Silicate taconite is the name used for virtually magnetite-free sections of the cherty-textured iron-formation (Figure 7). Slaty taconite is generally lean in magnetite, so modifiers are mainly words describing the color, and therefore the probable ratio of carbonate to iron silicate. For example, a black slaty taconite would contain mostly iron silicate and little chert or carbonate. A brown slaty taconite would contain more carbonate and chert with little iron silicate (White, 1954, p. 14). As shown by the stratigraphic column in Figure 8, the Biwabik Iron Formation is underlain by the Pokegama Quartzite (i.e., Pokegama Formation) and overlain by the Virginia Formation.

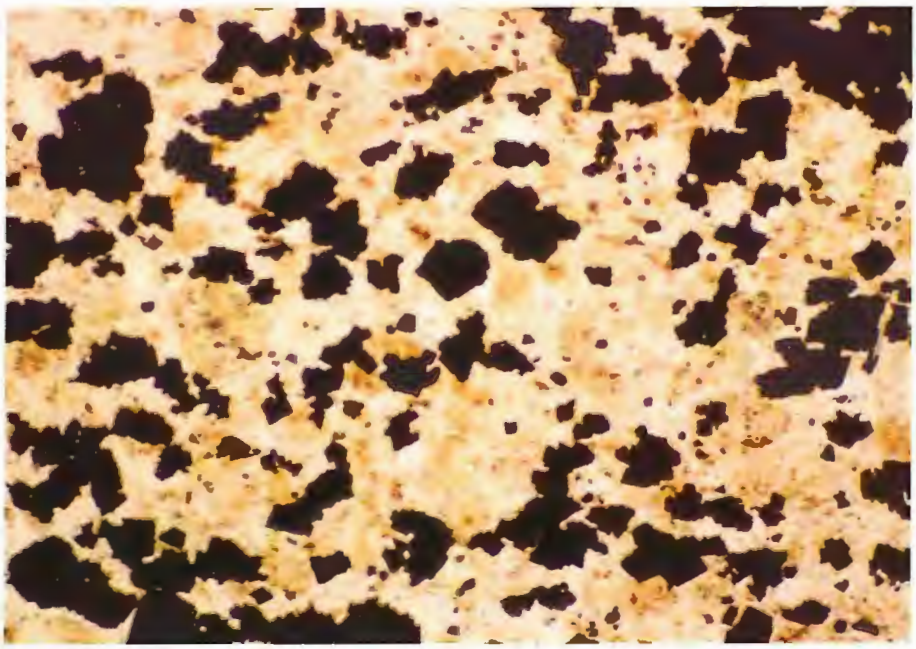

Figure 6. Cherty taconite. Aggregates of magnetite (black) are disseminated in a matrix of chert (clear), carbonate (light brown) and minor iron silicate (dark brown). Plane light. Field of view is 2.5 mm wide. Sample numbers for photomicrographs are listed in Appendix I.

Pokegama Formation:

The contact between the Pokegama Formation and the overlying iron-formation is conformable and locally gradational with interbedded quartzite, iron-formation, chert, and stromatolitic chert (Morey, 1972). A weathered exposure at Minntac shows the top of the Pokegama to be greenish-colored and chlorite-rich. Also near the top of the unit

are thin interbeds of dark grey to tan chert, exposed in angular fragments at Minntac. Jasper, laminated hematite, and intraformational conglomerate are found near the contact of the quartzite with the iron-formation. At Minntac, mounds of Pokegama quartzite are covered by even thicknesses of stromatolite horizons in the iron-formation, suggesting formation in tidal channels. This observation supports the idea that the iron-formation was deposited on a marine tide-influenced shelf (R. Ojakangas, 1983 and 1996; Simonson and Hassler, 1996; G. Ojakangas, 1996) as evidenced by tidal laminations, facies relations, texture and mineralogy.

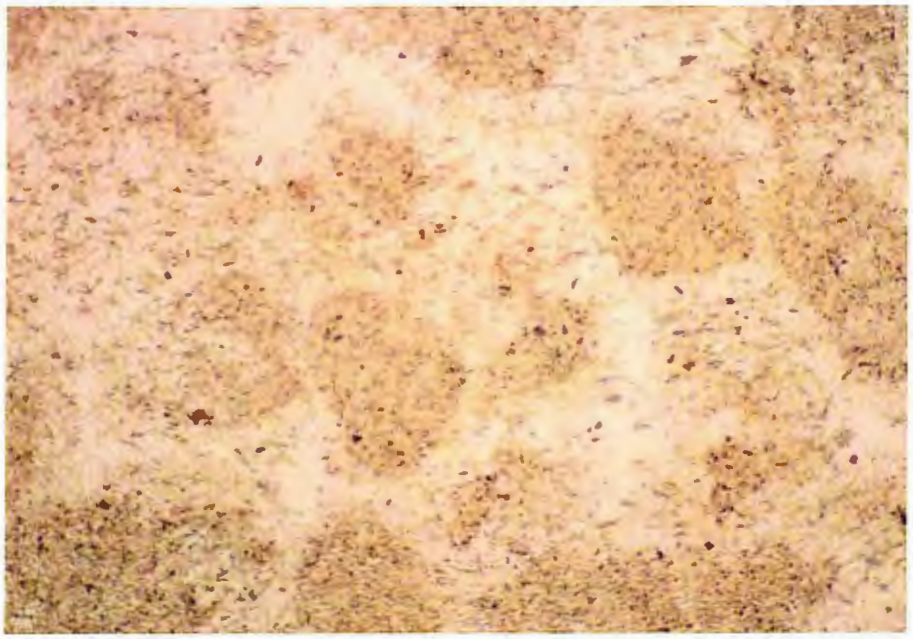

Figure 7. Silicate taconite. Granules of platy minnesotaite mixed with chert are being replaced by radiating minnesotaite. Magnetite content is minor. Plane light. Field of view is 2.5 mm wide.

In a more extensive study of outcrops and core of the Pokegama, Morey observed that the color of the quartzite ranges from white to green to pink. The thin-bedded quartzite is feldspathic and intercalated with micaceous, quartzose argillite. (Morey, 1972).

Heavy mineral studies indicate that the source of the Pokegama is the Giant's Range Batholith to the north (Morey, 1972). This fits the interpretation that the source of the terrigenous clastics in the Pokegama was from the Archean rocks to the north. The

Pokegama is interpreted as a tidal marine deposit (R. Ojakangas, 1983 and 1996, G. Ojakangas, 1996). Walther's law of succession of facies states that "the various deposits of the same facies-area and similarly the sum of the rocks of different facies-areas are formed beside each other in space, though in a cross-section we see them lying on top of each other" (Boggs, 1995, p. 501). Therefore, one can interpret that the Biwabik Iron Formation was also deposited in a marine setting beside the quartzite (R. Ojakangas, 1983).

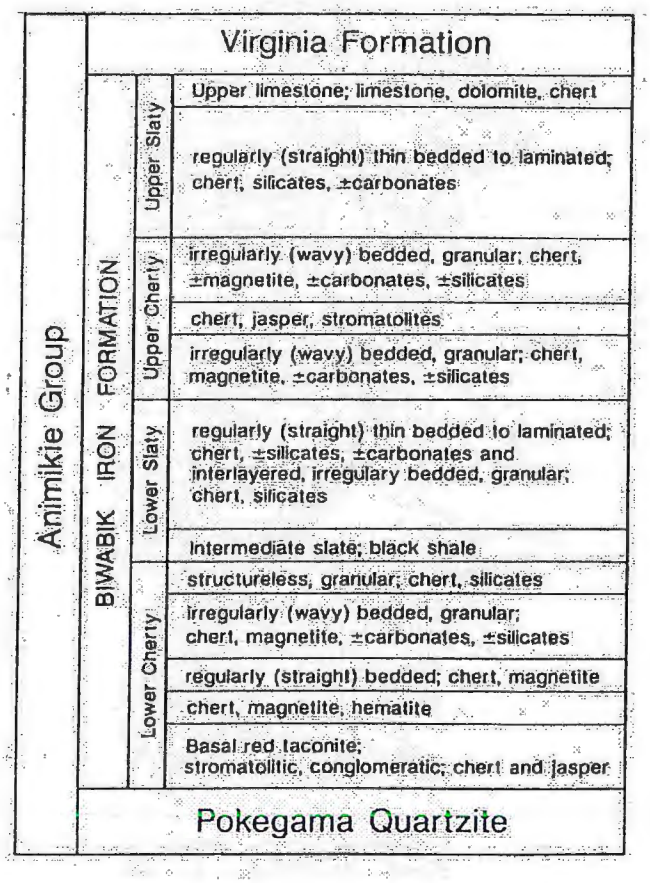

Figure 8. Generalized stratigraphic succession of the Biwabik Iron-Formation. From Morey, 1983

Virginia Formation:

The Biwabik Iron Formation is conformably overlain by interbedded carbonaceous shale, mudstone, argillaceous siltstone, and fine-grained feldspathic greywacke of the Virginia Formation. The contact indicates a change from chemical

deposition to terrigenous clastic deposition in the Animikie Basin. Lean iron-formations have been documented within the Virginia Formation, suggesting that the depositional change was gradual. There are no natural outcrops of the Virginia Formation, but it is interpreted to be continuous with the Thomson Formation of east-central Minnesota. Studies of greywacke within the Thomson Formation show graded bedding and sole marks, indicators of deposition by turbidity currents (Morey and R. Ojakangas, 1970).

Cretaceous:

The shoreline of the inland Cretaceous Sea reached the Mesabi Range and hematite-pebble conglomerates were deposited from erosion of oxidized iron-formation. Fossil evidence suggests the climate was subtropical (Austin, 1972).

Pleistocene:

Several advances and retreats of the Laurentide Ice Sheet indicate a much cooler climate dominated Minnesota during the Pleistocene. At least four glaciations occurring within the last 2 million years have been documented in the midcontinent region of North America (Patterson, 1998). Glacial till from the most recent glaciation obscures much of the Mesabi Range.

Auburn Pit:

To examine the texture and mineralogy of the iron-formation, 311 feet of core number 22L8, including the upper cherty, lower slaty, and lower cherty, were studied. Appendix II contains notes from the core log. The core, provided courtesy of EVTAC, was taken north of the Auburn pit. Figures 9 and 10 show a section of the core and the location where the core was obtained, respectively.

The Auburn pit was developed as an underground high-grade ore mine by the Minnesota Iron Company. From 1894 to1902, it produced 2,143,000 tons of ore (Crowell, 1927, p. 174). The Oliver Mining Company reopened the mine as a pit in 1951, producing an additional 7,000,000 tons of ore by the end of 1955 (Holway, 1956). From 1999 to 2001, Auburn Minerals extracted the remains of the high-grade ore.

The Auburn mine is located on the north side of the Eveleth anticline near the center of the Virginia Horn. Iron-formation in this area strikes northeast and dips about 10 degrees to the northwest (Holway, 1956). High-grade ore was concentrated along an axis 915 m long. The pit is 150 m wide and up to 80 m deep, exposing the Lower Cherty-Lower Slaty contact. Even the top of the underlying Pokegama Formation was exposed prior to flooding and dumping. Slump features from removal of silica via hydrothermal solution are visible on either end of the pit. About 6 m of greyish-brown bouldery till covered the top of the iron-formation (Holway, 1956). Figure 10 shows the mine in plan view.

Figure 9. Photo of one-inch diameter core from hole 22L8, approximately located at 365250 N, 214200 E.

The southwest wall of the Auburn mine is oxidized, and original depositional features are obliterated by the formation of oxidation products such as geothite. The northeast wall is fairly unoxidized and shows chert nodules, jasper granules, and cross-bedding in the cherty iron-formation. The lower slaty is generally evenly bedded with wavy or straight beds. Both cherty and slaty horizons are intermixed.

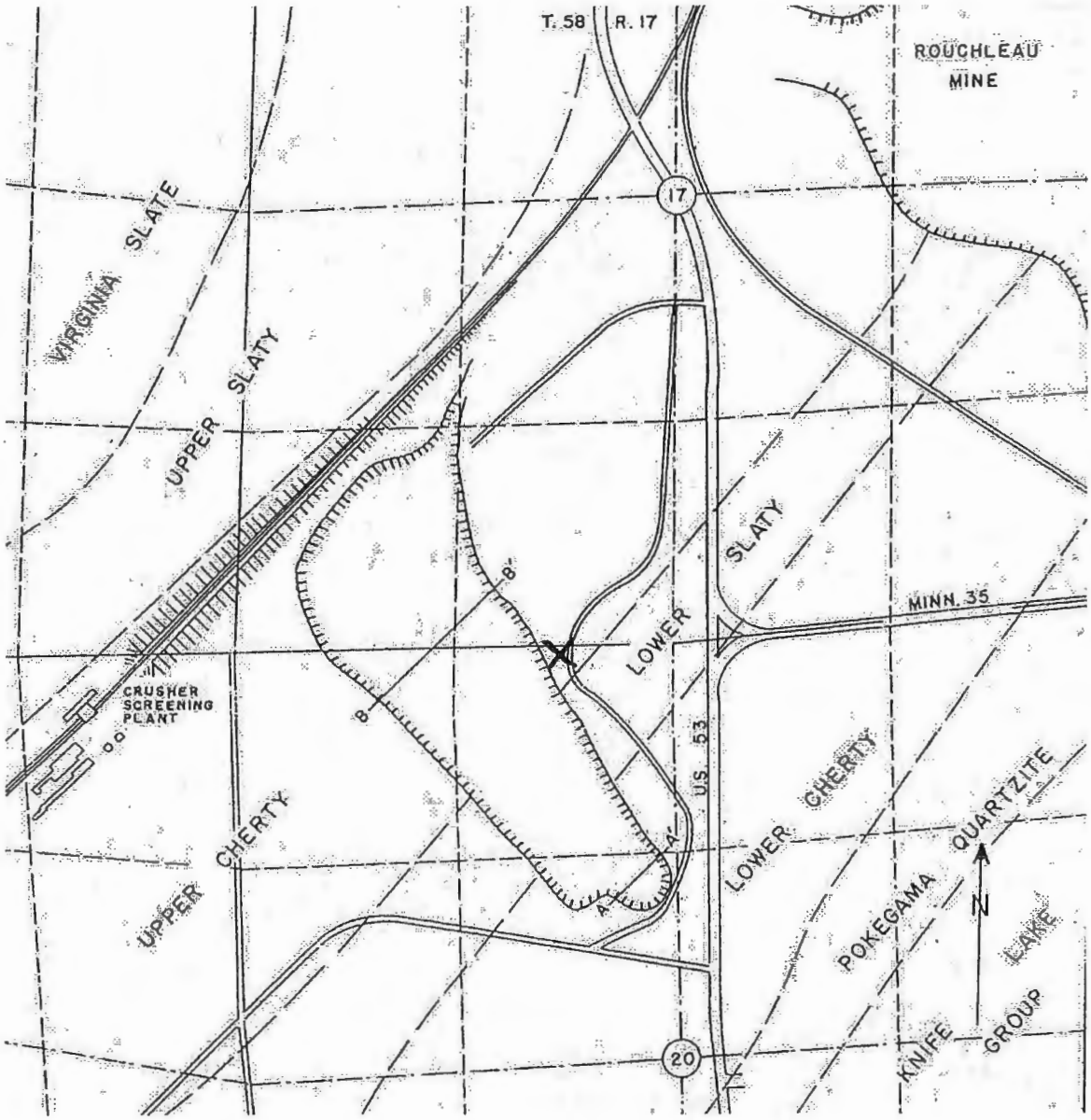

Figure 10. Geologic map of Auburn mine and vicinity. Approximate location of core 22L8 indicated by X. From Holway, 1956.

Methods for determining mineralogy:

A 311-foot long core, from drill hole number 22L8, drilled northeast of the Auburn pit, was logged to note color, texture, and mineralogy. A total of 39 samples of the core were taken for thin sectioning, approximately one every ten feet. Appendix III contains stratigraphic intervals and photocopies of the thin sections. Heels from the thin

sections were ground into powder and x-ray diffraction was used to identify predominant minerals. Powders from 13 thin sections were x-rayed.

X-ray diffraction (XRD) is an analytical technique that uses the interference patterns of x-rays scattering off of crystalline materials. As each mineral has a unique crystalline atomic structure, each mineral will produce a unique graph of x-ray intensity versus scattering angle. Mineral identification is possible by comparing the XRD pattern of an unknown mineral to a library of known patterns.

For rocks, XRD may be used to identify the main mineral constituents. Minor minerals are present in relatively miniscule amounts, minimizing the chance that they will show up in the diffraction pattern. If minor minerals do contribute to the diffraction pattern, it is likely that the peaks will not be intense enough to stand out from the background noise of the graph. Therefore, XRD analysis of whole-rock powders is only practical for identifying the major minerals in a rock.

Samples from drill hole 22L8 were analyzed using an XRD instrument manufactured by Philips Analytical. The XRD instrument was located at the University of Minnesota, Duluth. It produced K-alpha radiation and was set-up for continuous, measured scanning from 5° (2Theta) to 65° (2Theta). Step size was 0.0200° (2Theta), with 1.20 seconds per step. Each scan took approximately one hour. Resolution of peaks was not improved by using longer scan times. The incident beam mask was 15mm and 1° slits were used for the divergent and anti-scatter slits.

Using software developed by Philips Analytical in the X'Pert suite, called X'Pert Graphics and Identify, XRD patterns were compared with a database of diffraction patterns to identify possible mineral matches. The computer produced a list of possible mineral matches, along with a score corresponding to how well a given mineral's peaks matched the peaks in the XRD pattern. General mineral species were identified using the polarizing microscope (e.g. carbonates and iron silicates) and then the XRD pattern was helpful in determining the types of carbonate or iron silicate present.

The main minerals identified using x-ray diffraction in the cherty iron-formation include chert, minnesotaite, talc, greenalite, siderite, ankerite, magnetite, and stilpnomelane. Additional minerals identified in thin section include chlorite, hematite,

pyrite, and apatite, as well as possible carbonaceous material. X-ray diffraction analysis of the slaty iron-formation showed stilpnomelane, siderite, greenalite, minnesotaite, and chert. Minor magnetite, hematite, chlorite, pyrite, and carbonaceous material were found in the slaty iron-formation from thin section analysis. French (1973) and LaBerge (1964) have worked to determine primary diagenetic and secondary diagenetic mineralogies of iron-formation with respect to the original precipitates and the mechanism for deposition. French (1973) defined primary minerals as those having primary textures that are not visibly replacing pre-existing phases. Secondary minerals appear to be replacing or reacting with other minerals. LaBerge (1964) noted that primary minerals have a uniform fine grain size, appear to have been individual particles (or are a coating on primary particles), and are closely related to (or define) primary features such as bedding, granules, and chert spheres.

Mineralogy:

An unpublished report from EVTAC indicated the most abundant minerals in the Biwabik Iron Formation at the Thunderbird North Mine as determined by geochemical analysis and XRD of a composite sample (including 148 samples from four drill holes) are: Quartz, 14.64%; stilpnomelane, 14.24%; magnetite, 13.05%; siderite, 12.05%; minnesotaite, 11.85%; ankerite, 11.85%; talc, 7.97%; hematite, 5.28%; and greenalite, 4.68%. The following are observations from hand sample, thin section, and XRD analysis of core 22L8.

Iron Silicates:

Greenalite

Greenalite, $Fe_3^{+2}Si_2(OH)_4$, is a dark olive green in hand specimen. It is fine-grained and pale green to olive in plane light. The sub-microscopic grains are so concentrated that the mineral appears isotropic under crossed polars. The isotropic character distinguishes greenalite from platy minnesotaite (Gruner, 1946, p. 9). Greenalite is found in granules as well as in masses in the slaty iron-formation. LaBerge

(1964) noted that it might be disseminated as a dusty pigment in chert. Some greenalite granules contain equal proportions of chert and greenalite.

Within granules, greenalite is often found separated into spherical forms, each about 0.03 mm in diameter. LaBerge (1964) found variable amounts of chlorite intimately intergrown with the greenalite on a microscopic scale. Recently, Morey found microprobe evidence of chlorite minerals, specifically the iron-chlorite, chamosite (personal communication, R. Ojakangas, 1999). My own x-ray analysis has suggested that the mg-rich chlorite, clinochlore, may be present. Clinochlore forms a solid solution with chamosite. Clinochlore shows up in the same samples that have greenalite. As their optical properties are similar, it is virtually impossible to discern between the two optically. It may be the case that they are intermixed. In thin section it appears that some granules contain chlorite-rich, optically oriented patches in otherwise isotropic, fine-grained greenalite. Some of these patches may indicate the presence of stilpnomelane. Greenalite appears to be replaced by minnesotaite and magnetite (Figure 11).

Greenalite is assumed to be primary based on its fine grain size, the tendency to be replaced, and the appearance in granules and masses that define bedding (LaBerge, 1964).

Minnesotaite

Minnesotaite, $(Fe^{2+}, Mg)_3Si_4O_{10}(OH)_2$, is greenish gray in hand specimen. It was named by Gruner (1944) for Minnesota, the state where the mineral was discovered. Crystals occur in two distinct habits: microscopic plates or needles. Though no visual distinction was made between minnesotaite and talc, talc showed up on x-ray diffraction patterns instead of minnesotaite in some of the samples that appeared to contain minnesotaite. Talc has also shown up on x-ray in samples that look like minnesotaite in thin section (Figure 12). Talc forms a solid solution with minnesotaite and is the mg-rich end member. All five samples with talc contain magnetite. Talc-containing samples were at footages 135, 161, 185, 210, and 228. Minnesotaite-containing samples were at footages 20.5, 64, 75, 111, and 149. Based on this observation, it appears that minnesotaite may be more common in the upper cherty, and talc more common in the

lower cherty. White fibrous veins, which may be talc, appeared in the lower slaty portions of the core and were noted during core logging. The mineral was not preserved in the thin sectioning process and there was not enough vein material available to create powder for XRD identification.

Talc has also been noted in previous studies of iron-formation. It is unclear whether the talc formed as a replacement of minnesotaite, or in place of minnesotaite, or as an alteration product of minnesotaite. French (1973) identified talc replacing
stilpnomelane in the Biwabik Iron Formation. Klein (1983) noted that ferroan talc is more common that minnesotaite in the Gunflint Iron Formation.

Minnesotaite needles are radiating or in sheaves and replace quartz, carbonate, and iron silicates. They may be found nucleating within a mineral, or at the junction of two minerals such as between magnetite and chert (Figure 13), greenalite and chert, or carbonate and chert. Needles of minnesotaite are clear to light green under plane light, or reddish if they are oxidized. Pleochroism is often not discernable, but minnesotaite is pleochroic with Z and Y = pale green, X = colorless, or very pale yellow (Gruner, 1944). Crystals exhibit high interference colors under crossed polars, with parallel extinction.

Platy minnesotaite forms fine-grained masses and has a felt-like appearance at high magnification. It is yellowish green to dark green in plane light. When these aggregates occur as granules, they are distinguished from greenalite only by their mottled appearance under crossed polars (Gruner, 1944) (Figure 14). In some sections the platy minnesotaite will grade into the larger, colorless needles (Figure 15).

Minnesotaite needles that obliterate bedding and replace platy minnesotaite are assumed to be formed by secondary diagenetic processes. Minnesotaite granules that resemble greenalite in plane light may well be primary, based on the fine grain size of the platy variety and the smooth granule outlines, with granules defining bedding.

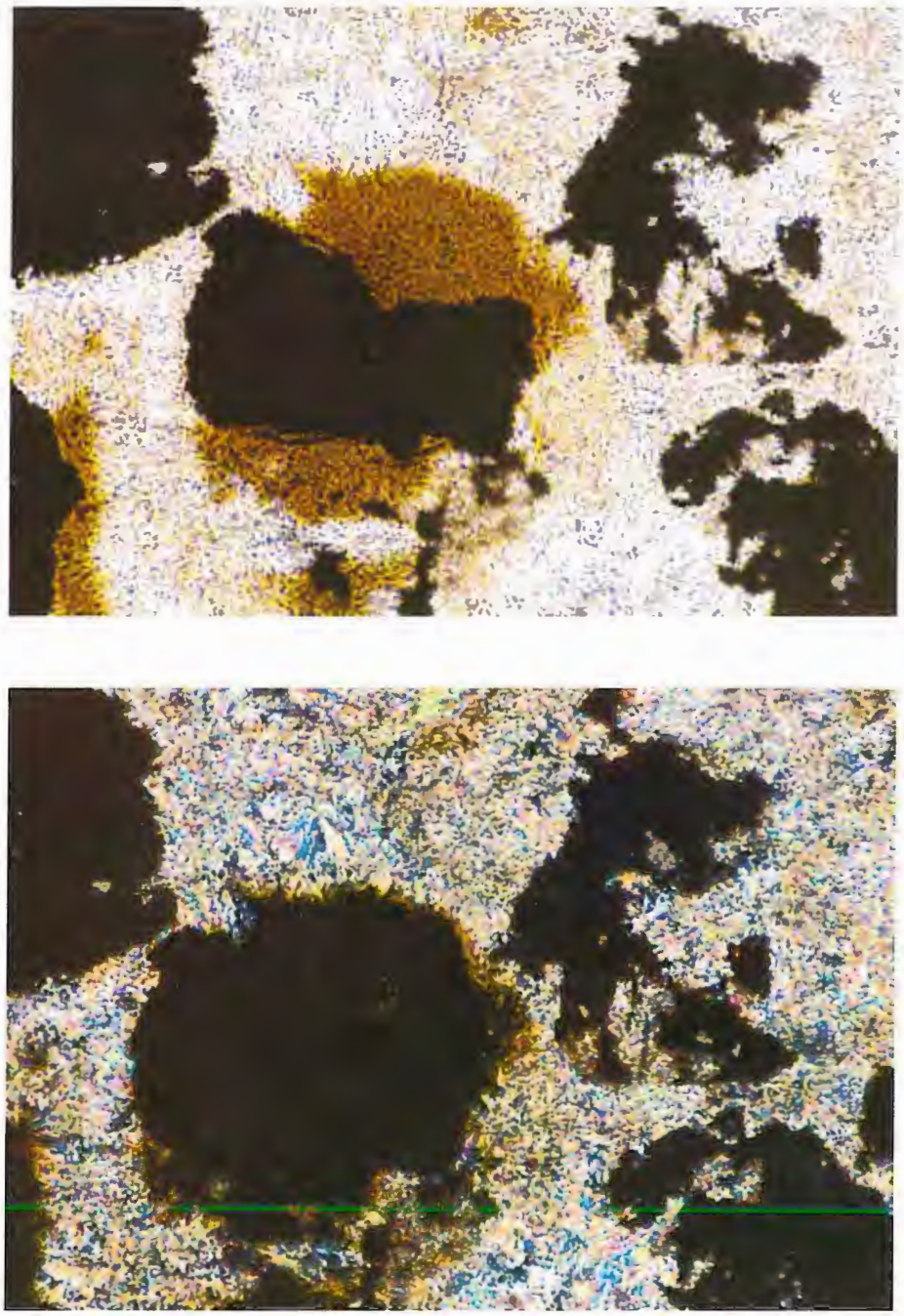

Figure 11. Greenalite (brown in plane light) is replaced by magnetite in a matrix of minnesotaite and chert. Upper view plane light, lower view crossed polars. Field of view is 1.0 mm wide.

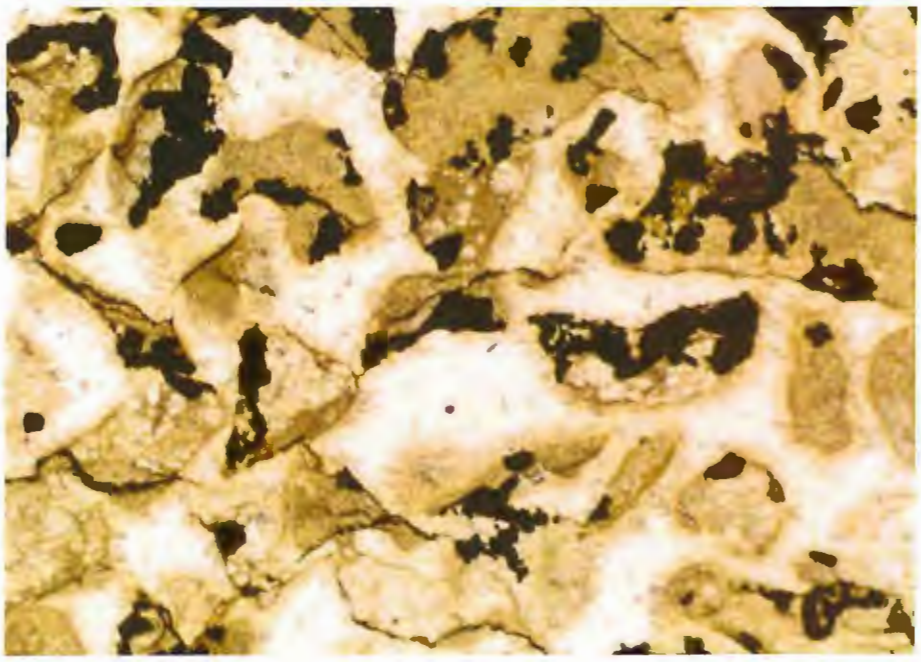

Figure 12. Granules and radiating crystals look like minnesotaite but were identified as talc by XRD. Chert cement. Magnetite is replacing parts of granules. Possible stilpnomelane seams between granules. Plane light. Field of view is 2.5 mm wide.

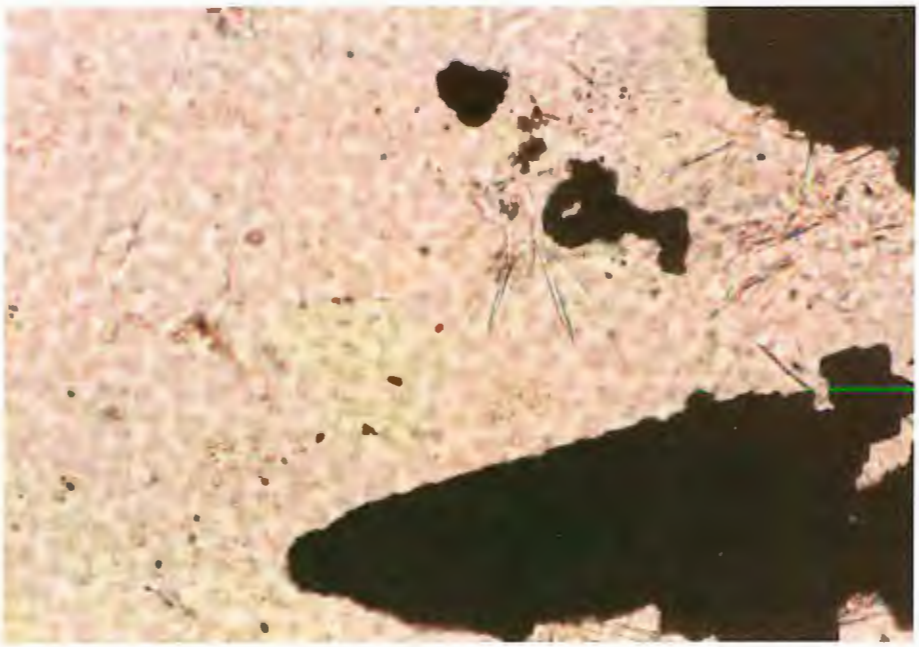

Figure 13. Needles of minnesotaite nucleating at the intersection of quartz and magnetite (center, right, and bottom right). Plane light. Field of view is 0.25 mm wide.

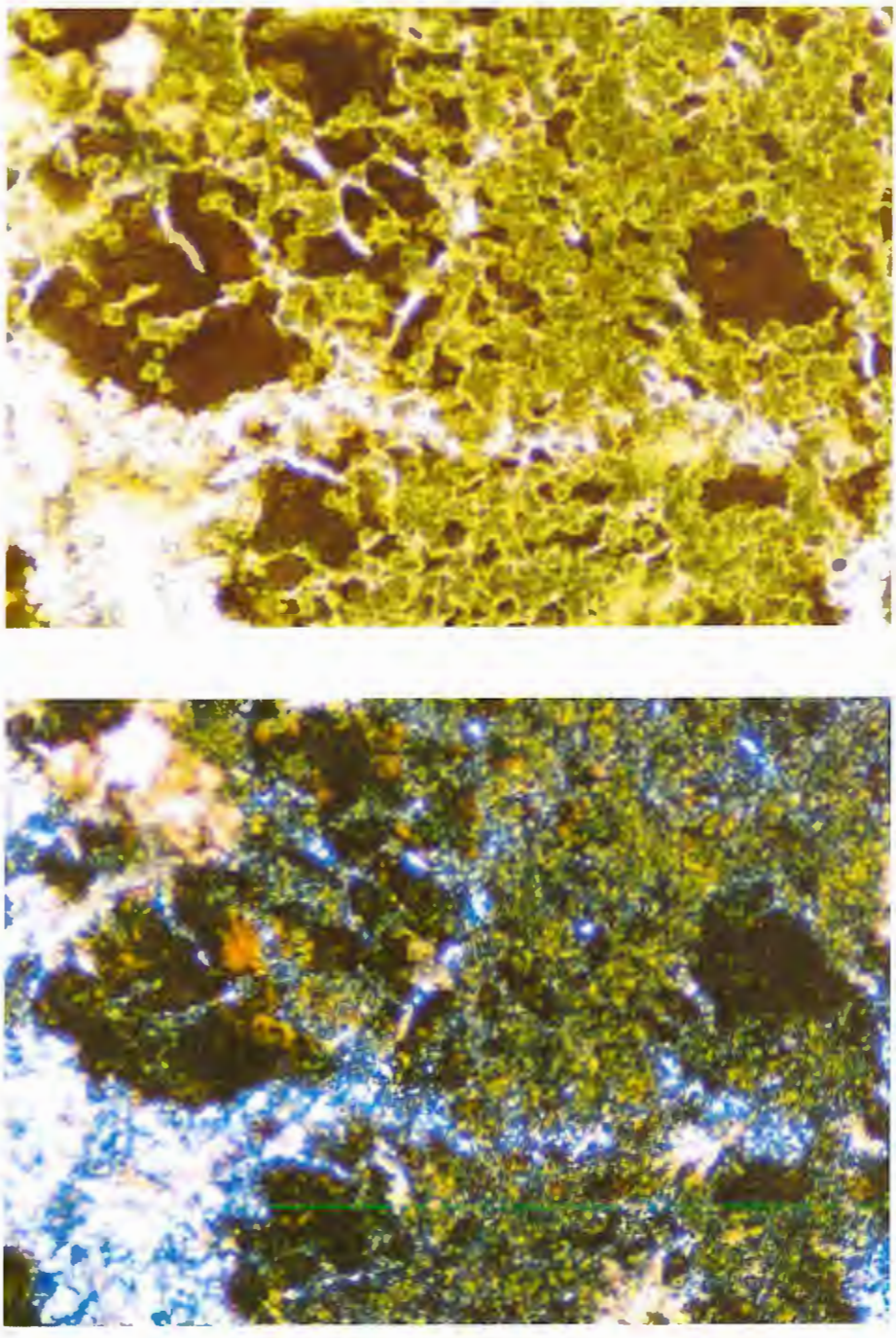

Figure 14. Platy minnesotaite as a mass of spheres. Darker brown patches may contain greenalite. Siderite is replacing iron silicate in chert cement. Note that dark spheres of similar size to minnesotaite spheres are seen in siderite and chert. Upper view plane light, lower view crossed polars. Field of view is 1.0 mm wide.

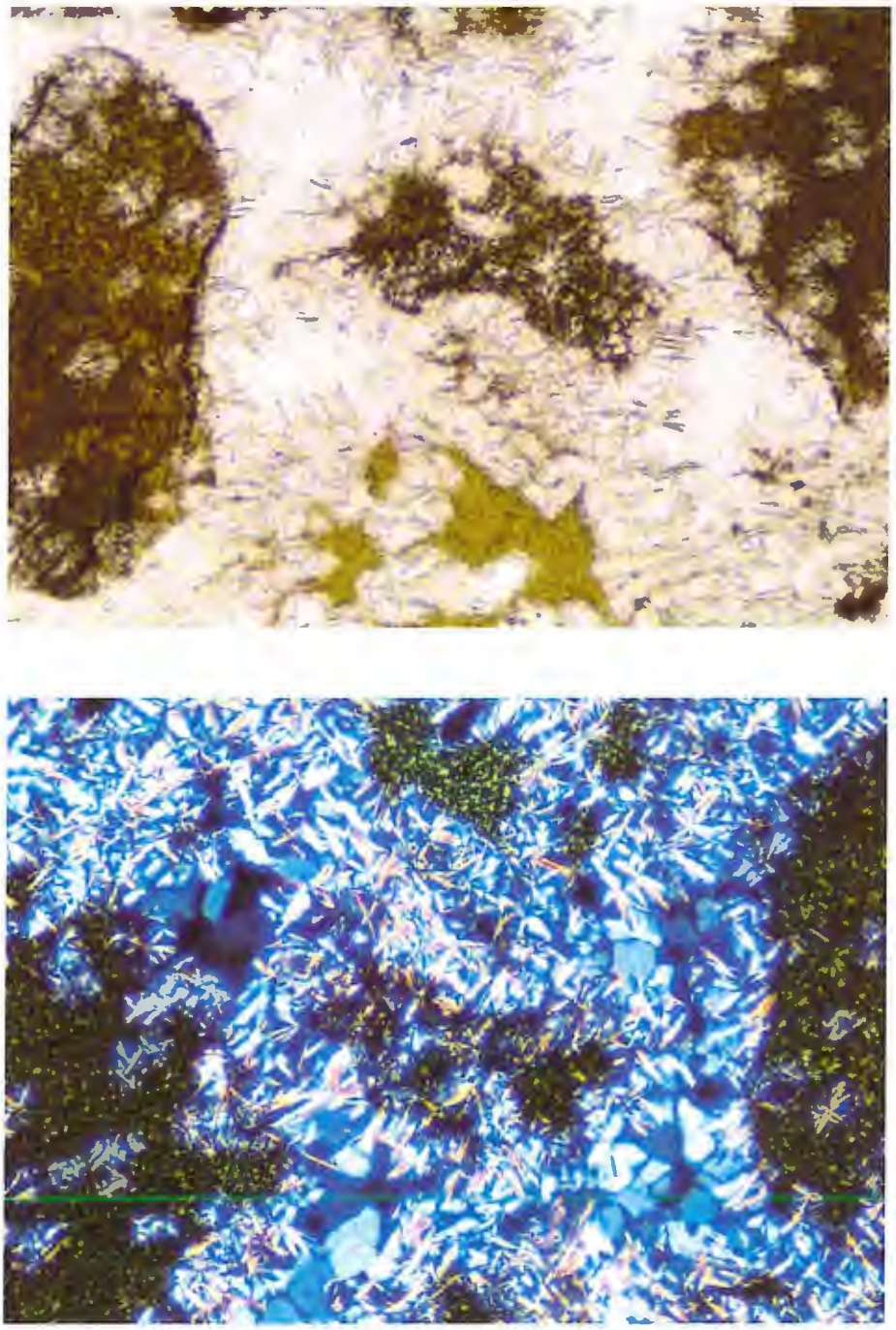

Figure 15. Minnesotaite granules containing spheres of chert. Minnesotaite needles have formed in chert and on the edge of granules. Chert cement. Opaque material unidentified. Upper view plane light, lower view crossed polars. Field of view is 1.0 mm wide.

Stilpnomelane

Stilpnomelane, (K, Ca, Na)(Fe^{2+}, Mg, Fe^{3+})$_8$(Si, Al)$_{12}$(O, OH)$_{27}$· nH_2O, is the third type of iron silicate found in the Biwabik Iron Formation. It occurs as foliated masses similar to minnesotaite needles, as well as in microscopic plates that are intermixed with the other iron silicates (Gruner 1946, p.14). Stilpnomelane is olive green to dark brown in plane light, and it is strongly pleochroic. Green varieties are pleochroic from yellow to olive green; the brown varieties are pleochroic from brown to black-brown.

Stilpnomelane is found in the granule-bearing phases of the cherty iron-formation (Figure 16), but is more abundant as masses in the slaty iron-formation (Figure 17). It tends to obliterate bedding in the slaty iron-formation as well as in the cherty iron-formation. Stilpnomelane in the slaty portions is very fine-grained and Gruner (1944) observed that it is hidden in dense, dark portions of the slaty rocks.

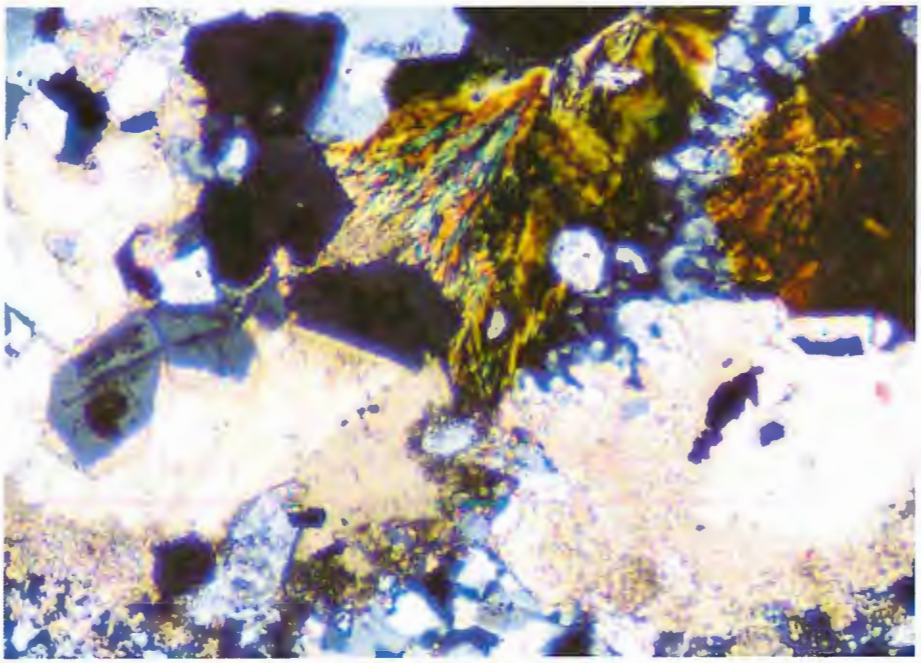

Figure 16. Fibrous iron silicate at top and right may be stilpnomelane. Note quartz crystals in carbonate. Chert cement. Crossed polars. Field of view is 1.0 mm wide.

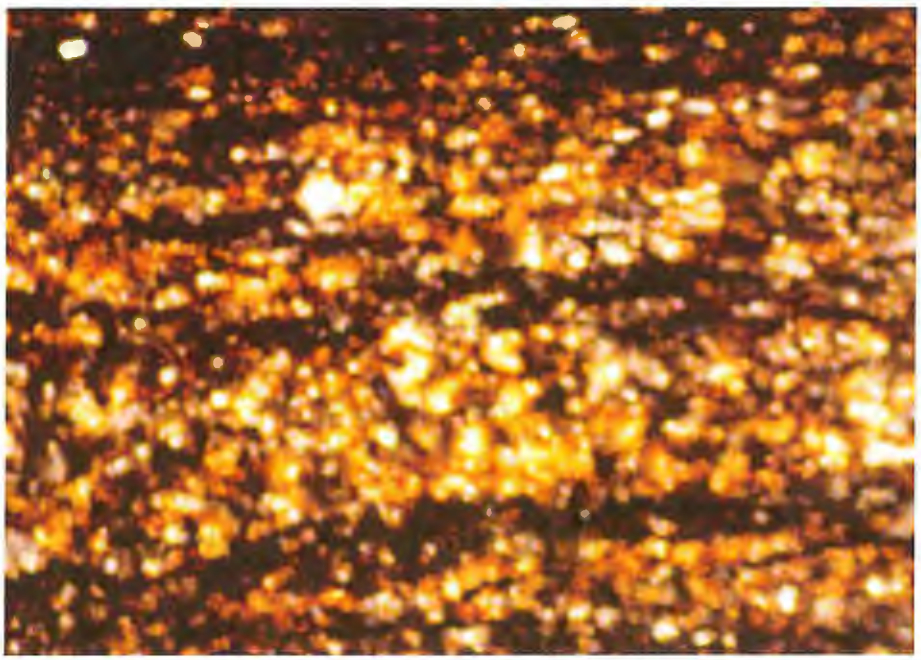

Figure 17. Stilpnomelane is present as dark seams in the slaty iron-formation, along with greenalite, siderite, and chert. Plane light. Field of view is 2.5 mm wide. Due to the extremely fine-grained nature of the slaty iron-formation, the rock appears dark in transmitted light and individual minerals could not be brought into a single plane of focus, thus imparting a fuzzy appearance in the photomicrograph.

Chert:

Chert, SiO_2, is the most abundant mineral in the Biwabik Iron Formation. In cherty taconite, it is present as cement (Simonson, 1987) between granules, partial and complete replacement of granules (Figures 18 and 19), bands, lenses, veins, and single crystals (Figure 20). In slaty taconite, it is present in lenses of granule-bearing iron-formation and in veins and occasional single crystals. It is colorless in plane light, although it may have a light brown tint under crossed polars caused by microscopic particles of other minerals or possibly organic material. It is commonly tinted when it forms granules (Figure 21). Gruner (1946, p. 18) thought the microscopic particles appeared to be in colonies, suggesting an organic origin. Occasionally, the particles outline 5-30 micron spherical forms similar in size and shape to those in greenalite. Chert has replaced as well as been replaced by carbonate and iron oxide minerals and displays a variety of growth textures (Figure 22).

Jasper is chert colored with hematite, Fe_2O_3, dust and is darker brown in color. Jasper layers become purple near magnetite-rich layers. The purple coloration is correlated with the presence of disseminated magnetite in the jasper, and in places with a coarsening of the grain size of hematite (LaBerge, 1964).

While quartz is the only pure silica mineral presently found in iron formations, Simonson (1987) suggested that a range of silica polymorphs from opaline to gelatinous silica to drusy quartz were all precipitated as primary cements. Microcrystalline quartz (i.e., chert) is assumed to be an early forming, secondary mineral (Simonson, 1987).

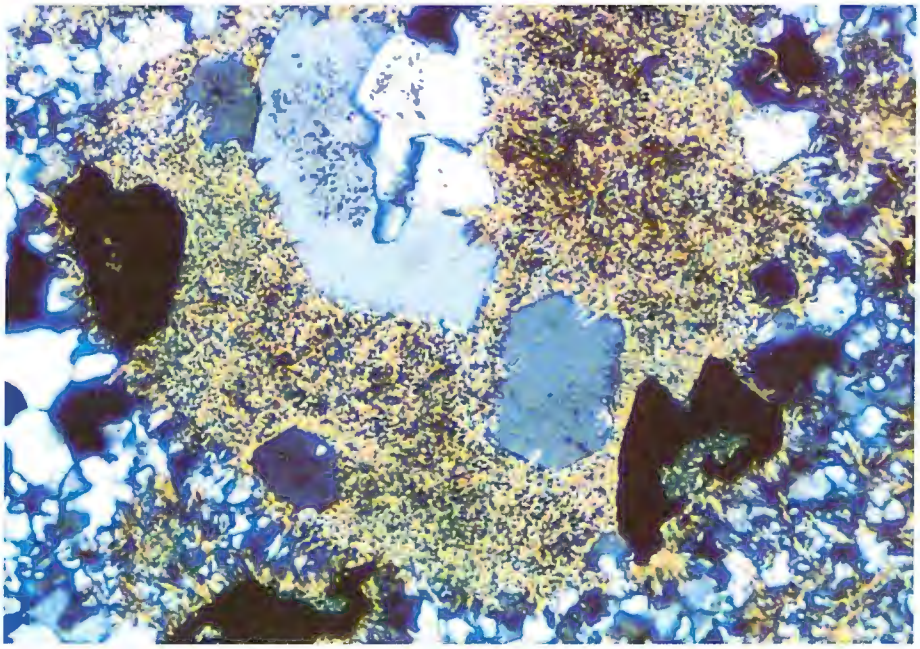

Figure 18. Euhedral quartz crystals in a granule replaced by needles of minnesotaite. Chert cement. Note magnetite in lower right of granule is surrounding platy minnesotaite. Crossed polars. Field of view is 1.0 mm wide.

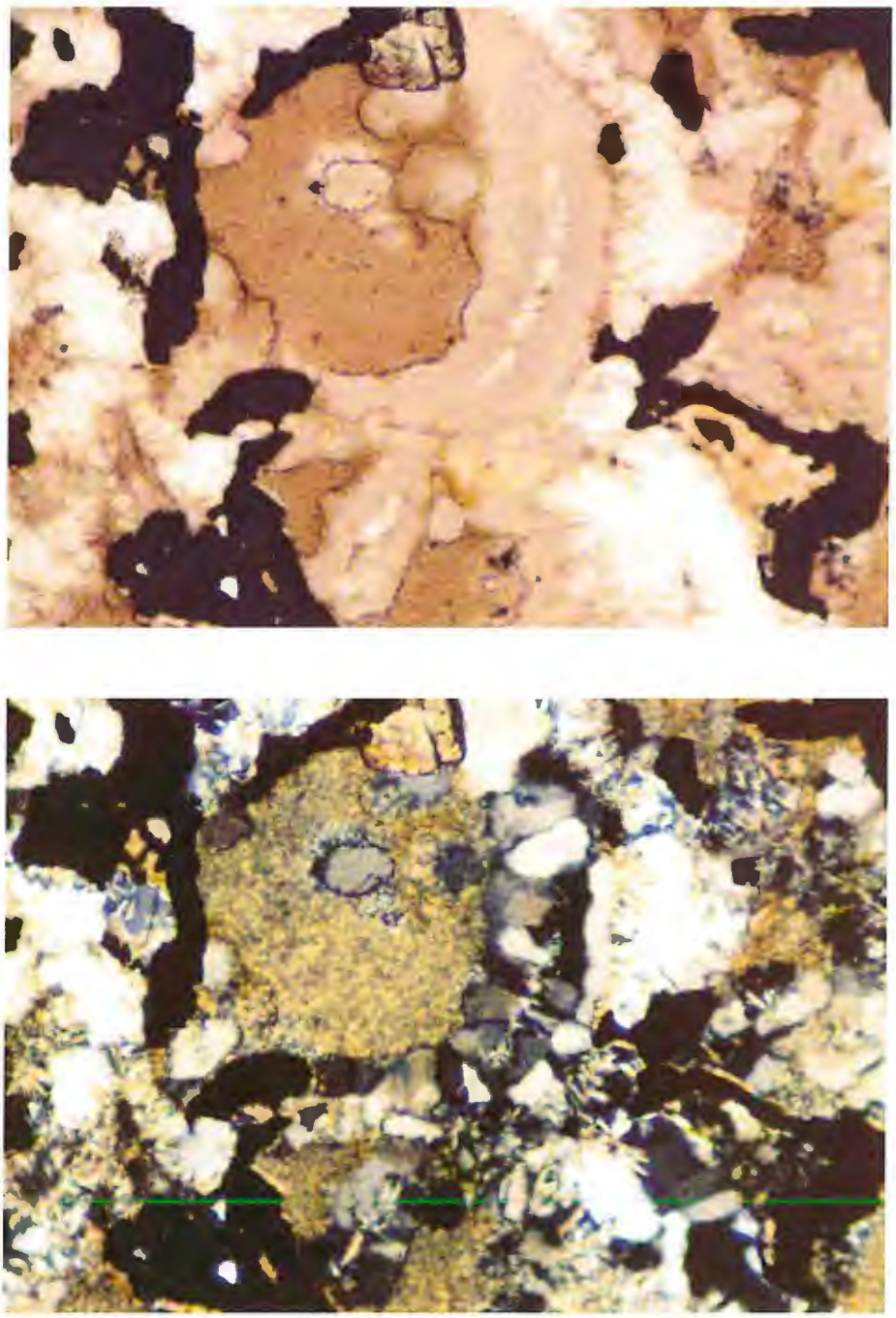

Figure 19. Brown chert growing perpendicular to iron silicate granule (center). Carbonate and magnetite and quartz replace iron silicate. Clear chert and needles of minnesotaite in cement. Upper view is plane light, lower view crossed polars. Field of view is 1.0 mm wide.

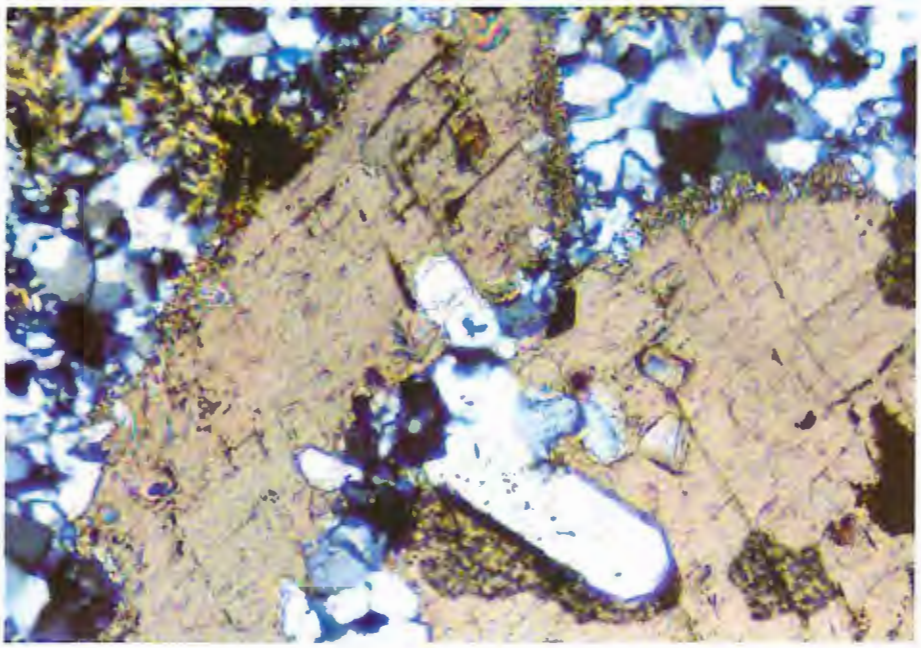

Figure 20. Euhedral quartz in carbonate. Chert cement with minor magnetite and iron silicate. Crossed polars. Field of view is 1.0 mm wide.

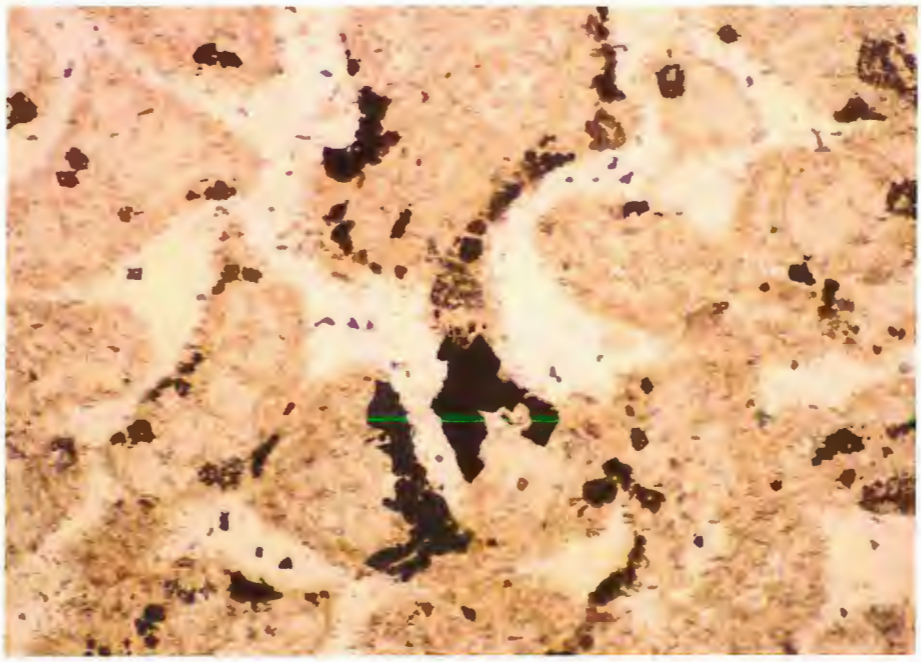

Figure 21. Chert granules (brown) replaced by needles of minnesotaite and magnetite. Cement is clear chert. Plane light. Field of view is 2.5 mm wide.

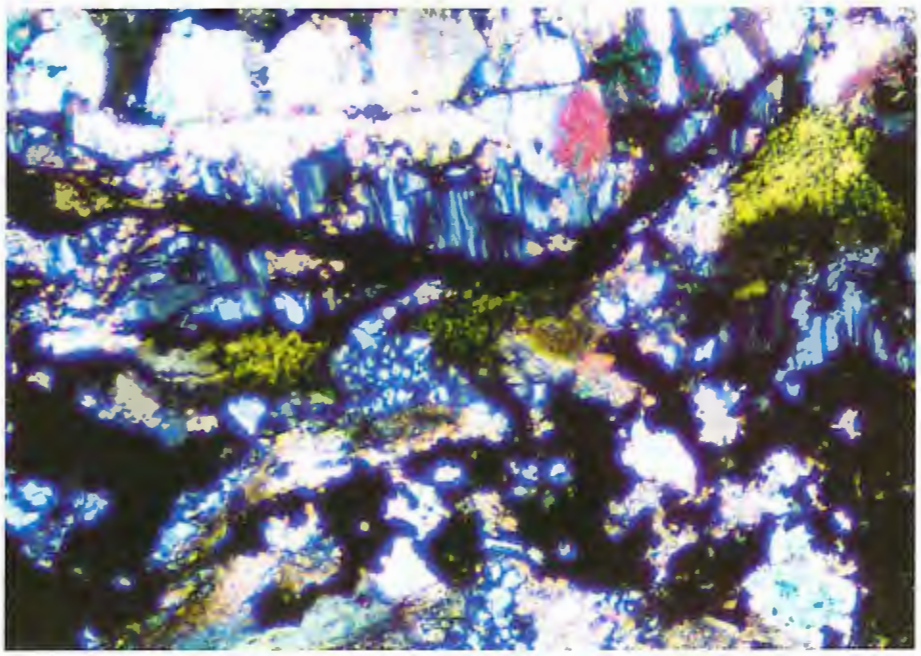

Figure 22. Chert growing perpendicular to magnetite and carbonate. Iron silicate granules (possibly chloritic due to the non-isotropic nature, fibrous extinction pattern, and color) and chert cement. Crossed polars. Field of view is 1.0 mm wide.

Iron carbonates:

Siderite

Siderite, $FeCO_3$, is slightly more abundant than ankerite in the Biwabik Iron Formation. It is greenish-grey to yellow-brown in hand specimen. Siderite is found in partings and granules in cherty horizons, and in masses in the slaty horizons. In plane light siderite is a clear, yellowish brown, and has high interference colors with translation gliding in coarse crystals (Gaines et al., 1997, p. 435). It may form coarse, interlocking crystals (Figure 23) or be in aggregates of small, spherical forms similar to the size and shape of the spheres in greenalite and chert (Figure 24). LaBerge (1964) measured individual spheres at approximately 0.05 mm in diameter. Some spheres contain an opaque dust. The crystalline and spherical habits may grade into one another (Winter and Knauth, 1992).

Granules of siderite may be composed of small, spherical grains of random orientation, or crystals forming optically continuous patches, or granules containing coarse, interlocking crystals (Winter and Knauth, 1992). Due to these various stages of

recrystallization observed in the siderite granules, LaBerge (1964) stated that the granules were derived from fine-grained layers of siderite. These layers may have been fragmented, or individual siderite grains may have aggregated into granule form. Coarse siderite may be a replacement of earlier granules. Layers of siderite do not contain much chert, but siderite has been replaced by and replaces chert.

Siderite is assumed to be primary due to the spherical nature of the particles, the close association with other minerals assumed to be primary (Figure 25), and its dominance as a carbonate species in iron-formation (LaBerge, 1964).

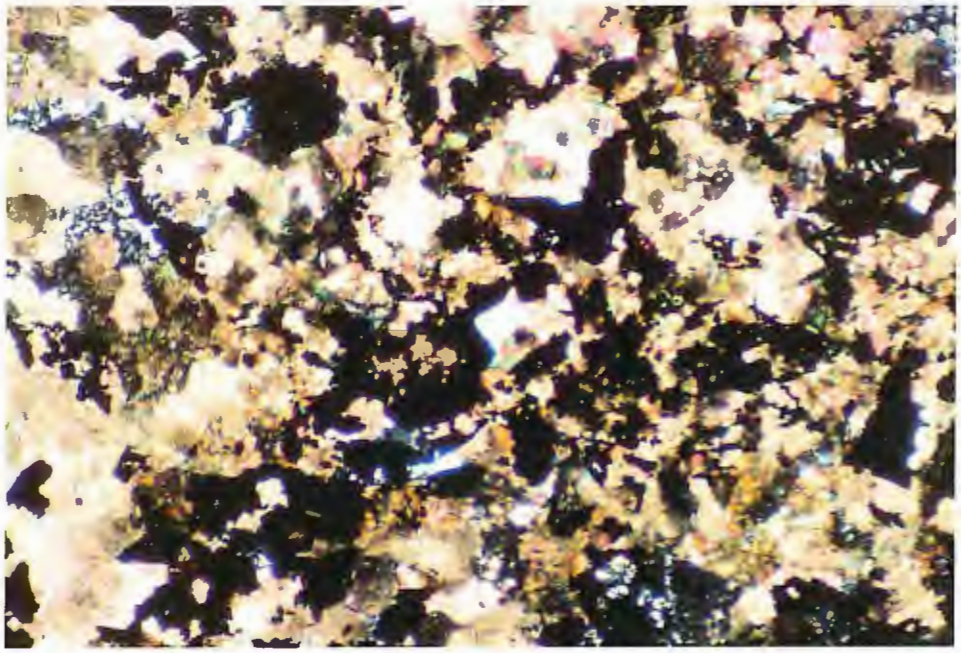

Figure 23. Fine-grained siderite replaced by coarse-grained siderite. Magnetite associated with siderite. Minor chert cement. Crossed polars. Field of view is 2.5 mm wide.

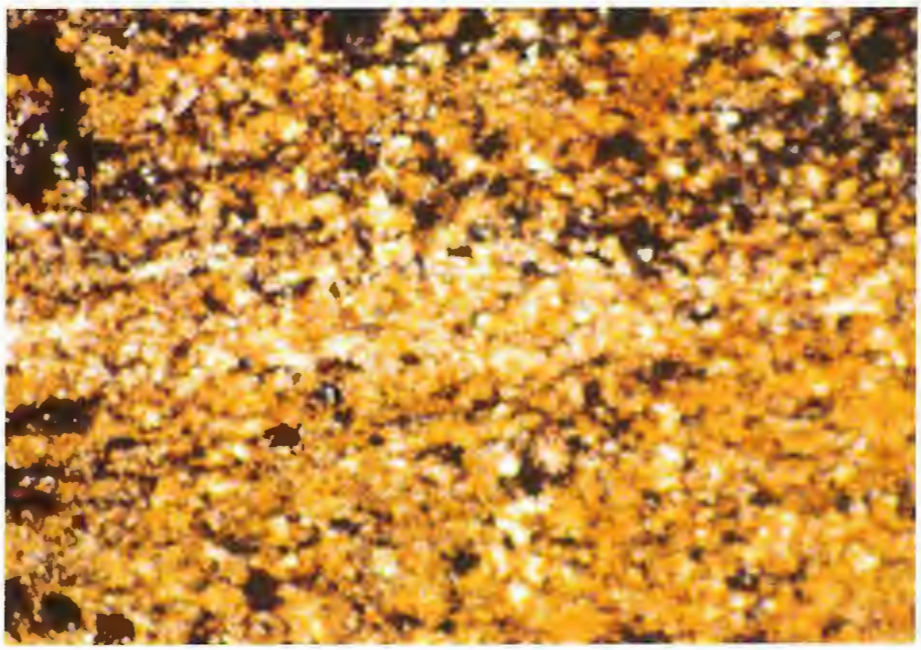

Figure 24. Siderite-rich slaty iron-formation. Plane light. Field of view is 2.5 mm wide.

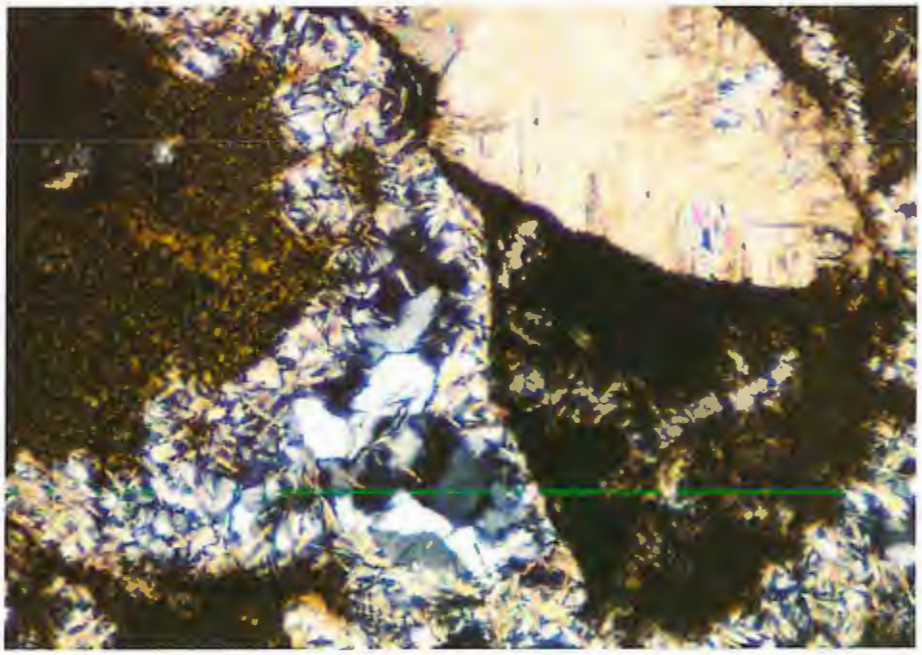

Figure 25. Coarse grain of siderite associated with cracked greenalite granule. Greenalite grades into an opaque seam on left side of siderite. Minnesotaite granule (left). Chert and needles of minnesotaite in cement. Crossed polars. Field of view is 1.0 mm wide.

Ankerite

Ankerite, or ferruginous dolomite, $Ca(Fe^{2+},Mg,Mn^{2+})(CO_3)_2$ is not easily identifiable as different from coarse-grained siderite, except with x-ray diffraction. It has the same character as coarse siderite and virtually identical optical characteristics (Klein and Hurlbut, 1985, p. 415). It forms coarse interlocking patches and veins as well as single crystals replacing chert or iron silicates (LaBerge, 1964). It is closely associated with magnetite, which tends to radiate out from a center of ankerite. This forms circular and lensoid shapes, and is found in the cherty iron-formation (Figure 26). It is considered to be secondary due to the coarse crystal habit and the close association with magnetite (Winter and Knauth, 1992) (Figures 27 and 28). LaBerge (1964) considered that oxidation and decomposition of siderite may cause the formation of ankerite.

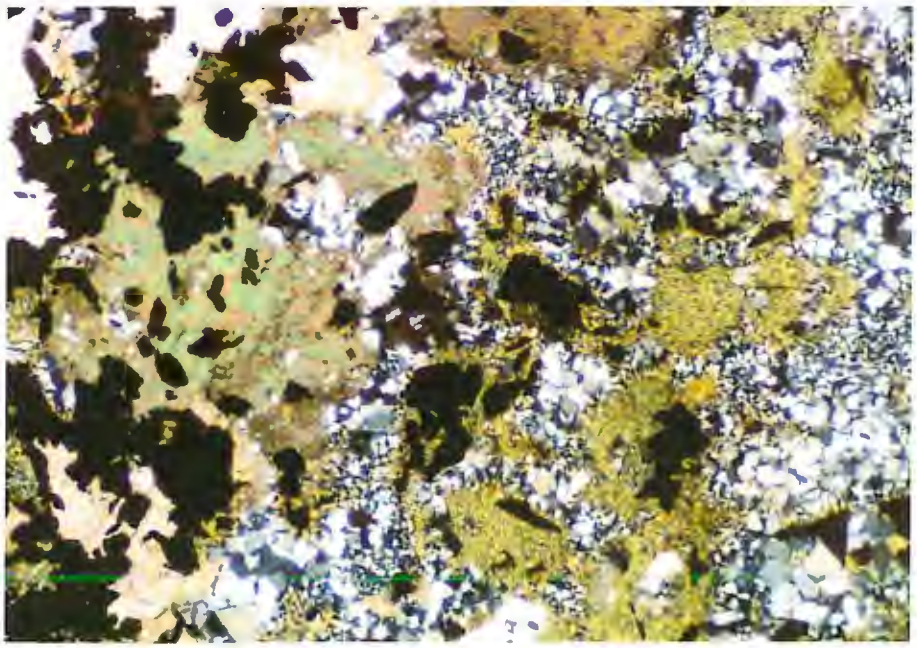

Figure 26. Ankerite (left) with magnetite. Chert cement with granules of iron silicate. Crossed polars. Field of view is 2.5 mm wide.

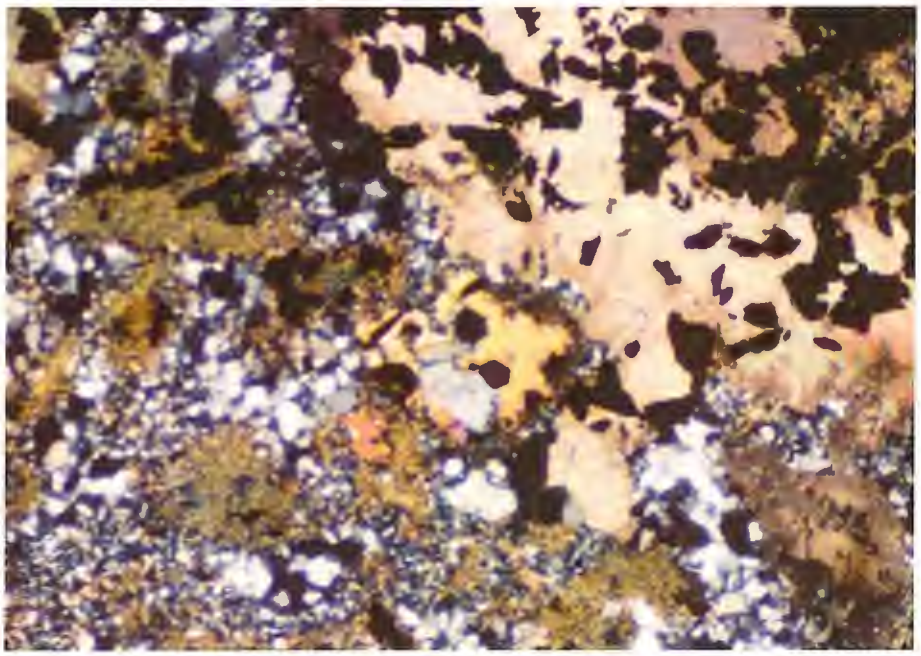

Figure 27. Ankerite (upper right) with magnetite. Chert cement with granules of iron silicate. Crossed polars. Field of view is 2.5 mm wide.

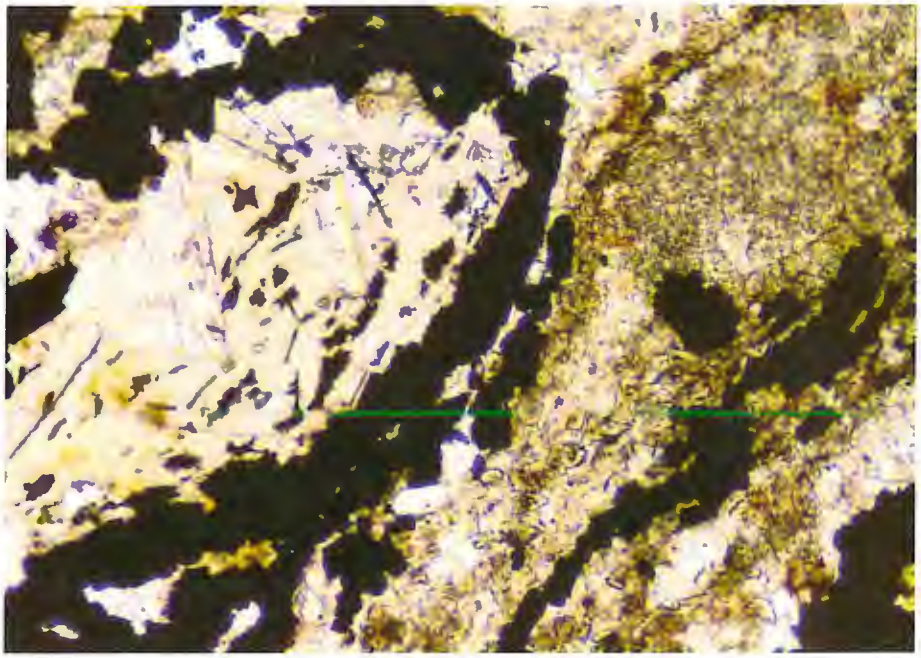

Figure 28. Ankerite and magnetite with minor chert. Plane light. Field of view is 1.0 mm wide.

Iron Oxides:

Magnetite

Magnetite, Fe_3O_4, is black with metallic luster and is strongly magnetic. It occurs as disseminated octahedra and as coarse aggregates of grains replacing iron silicates and iron carbonates (Figure 29). Magnetite is not present in all parts of the cherty iron-formation and it is not common in the slaty iron-formation.

In contrast to chert, siderite, and greenalite granules, magnetite crystals are not constrained by granule or bedding boundaries. It exhibits replacement textures and occurs in patches within or discontinuous rims around granules (Figure 30), as veinlets, as interconnected aggregates or clusters of aggregates, and as disseminated octahedra (LaBerge, 1964). In some cases, the magnetite was difficult to distinguish from carbonaceous material when the magnetite was fine-grained and disseminated. Gruner (1946) and LaBerge (1964) found that the size of individual crystals of magnetite is 30 to 100 microns, with aggregates over 1000 microns long.

Radiating minnesotaite, stilpnomelane, and ankerite are closely associated with magnetite (Figure 31). These associated minerals and the magnetite tend to obliterate granule outlines and layering. Magnetite is found in complexly intergrown aggregates of variable-sized crystals, unlike the uniform size and shape of the minerals generally accepted as primary (LaBerge, 1964). Magnetite has replaced iron silicate and carbonate minerals and does not appear to be replaced by any mineral. This evidence suggests that magnetite is secondary.

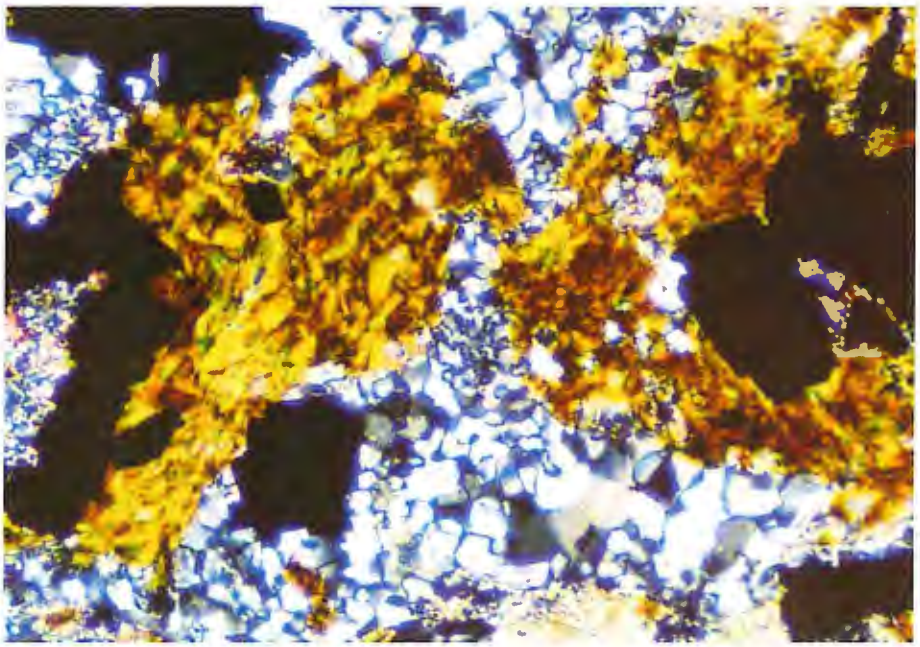

Figure 29. Magnetite associated with fibrous iron silicate. Chert cement with minor carbonate (bottom center and top right). Plane light. Field of view is 1.0 mm wide.

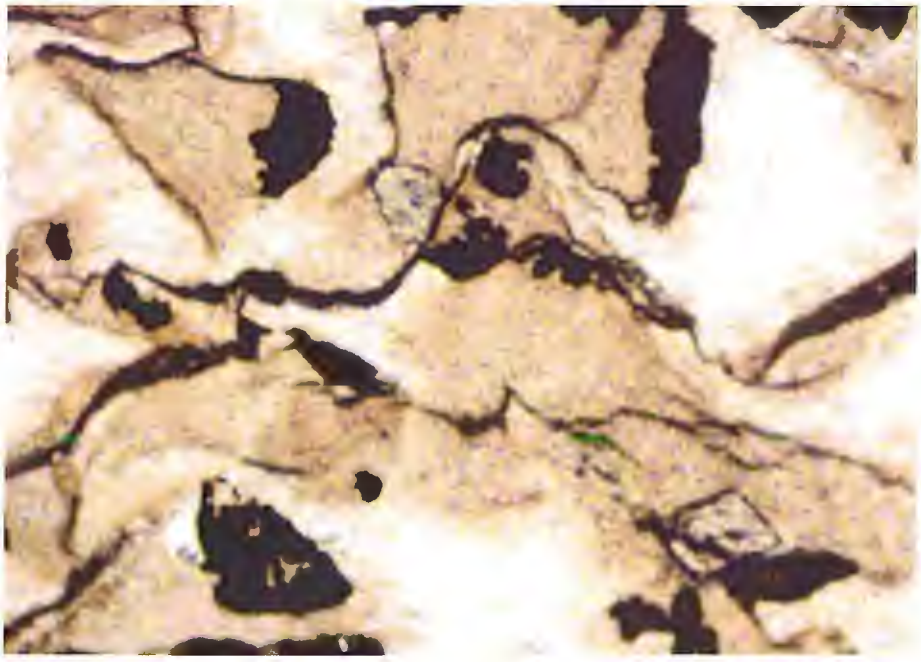

Figure 30. Magnetite in iron silicate granules. Stilpnomelane seams between granules. Minor coarse carbonate associated with iron silicates. Chert cement with needles of minnesotaite on edges of granules. Plane light. Field of view is 1.0 mm wide.

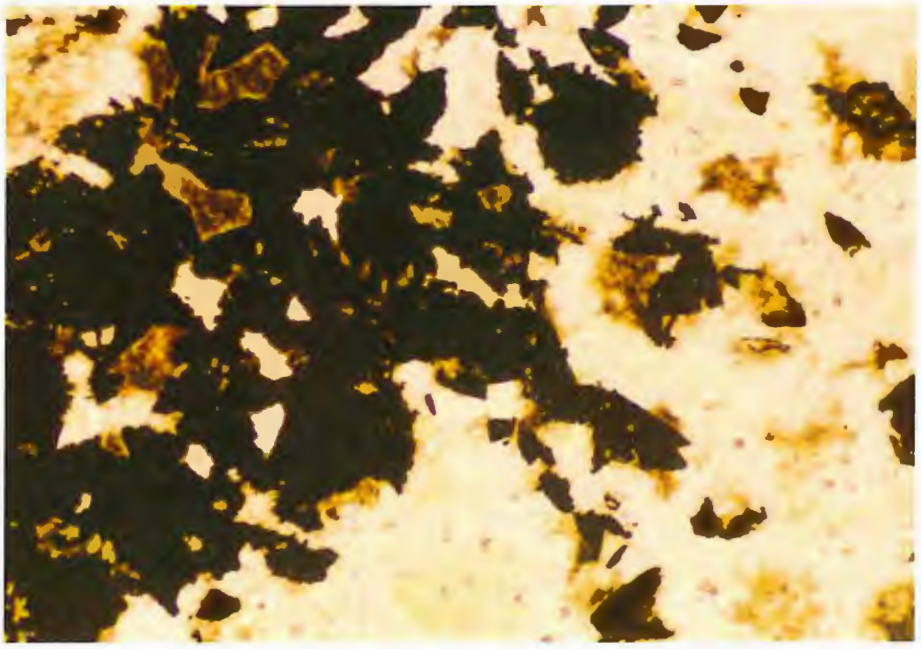

Figure 31. Magnetite forming a circular concentration (bottom right of circle is shown). Associated with carbonate and iron silicate. Chert cement. Plane light. Field of view is 1.0 mm wide.

Hematite

Hematite, Fe_2O_3, is found as minute crystals disseminated in chert (Figure 32), as well as in some oxidized portions of the slaty and cherty iron-formations. It is red in hand specimen and lends a purple color to chert to make jasper, such as in stromatolites. It is opaque with a red reflection. When found as inclusions in chert, it is assumed to be primary (LaBerge, 1964). In high grade ore pits where it has formed as an oxidation product of iron carbonate and iron silicate, it is secondary. Hematite did not show up on x-ray diffractograms, probably due to its low occurrence relative to the other minerals in the x-rayed powders.

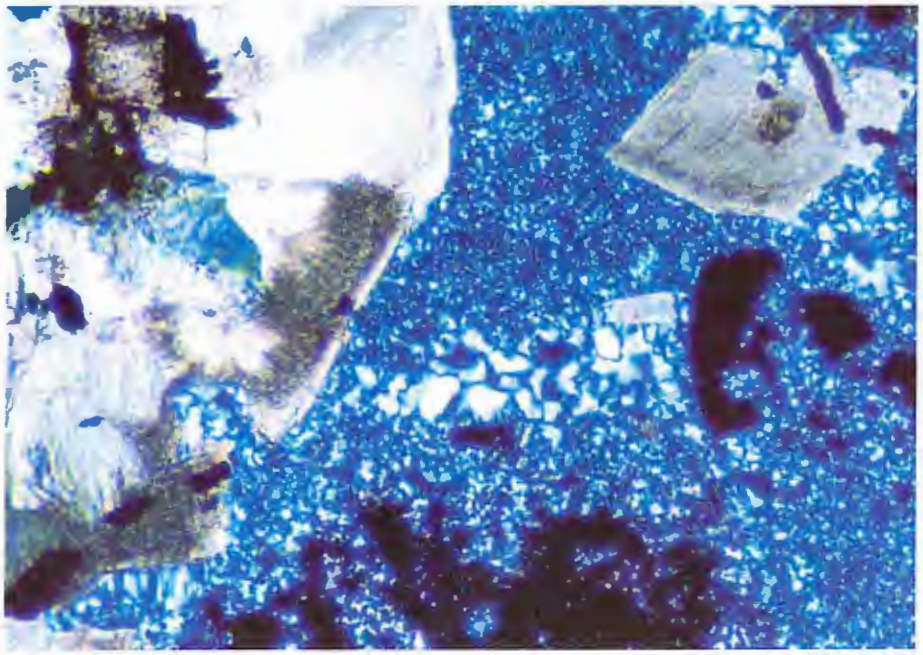

Figure 32. Concentration of hematite grains (bottom center) in a matrix of chert. Carbonate replacing chert. Larger opaque grains may be magnetite. Minor iron silicate surrounded by oxide mineral in carbonate. Crossed polars.
Field of view is 1.0 mm wide.

Other:

Pyrite

Pyrite, FeS_2, is yellow and metallic, making it easily visible in hand specimen as disseminated layers in the slaty iron-formation, as individual crystals in the cherty iron-formation, and as cross-cutting veins. Pyrite was only present in non-magnetic areas, with the exception of veins that cross-cut magnetite-rich areas. In thin section, the cubic crystals are associated with ankerite (Figure 33), possibly indicating that pyrite formed as a secondary mineral.

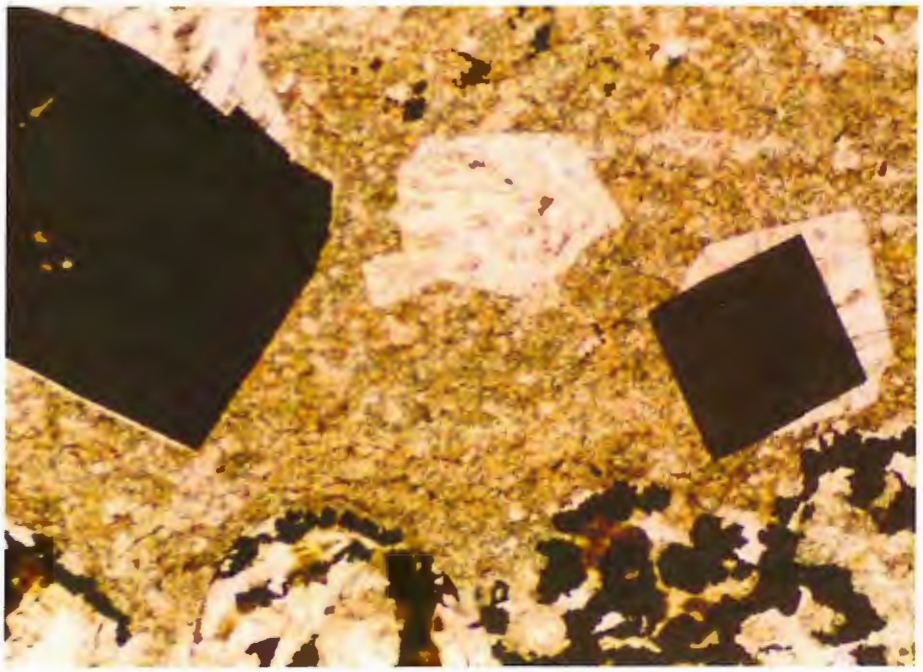

Figure 33. Pyrite cubes in a coarse crystalline ankerite layer. Magnetite forms a wavy layer below. Plane light. Field of view is 2.5 mm wide.

Apatite

Apatite is present in trace amounts. Although it did not show up on x-ray diffractograms, it is assumed to be fluorapatite, $Ca_5(PO_4)_3F$, due to its occurrence in other low grade pits of the Mesabi Range (Jongewaard, 1998). It is associated with magnetite and chert, forming prismatic crystals surrounded by magnetite. The crystals have low first order interference colors of greyish blue, and have a pitted surface (Figure 34). Crystals are length slow, which is inconsistent with a mineralogy text's description of apatite being length-fast (Gribble and Hall, 1992, p. 186). Juneau identified apatite in iron-formation and also found that it was length slow (1979, p. 119). Crystals have parallel extinction, but are too small to obtain optic figures. Due to the close association with magnetite, apatite may be a secondary mineral.

Apatite was found in the cherty iron-formation, at footage 149. This is located in the top of the Lower Cherty. Jongewaard (1998) has noted that this section of ore typically yields as much phosphorous in the concentrate as in the crude ore. This fits the interpretation that the mineral is apatite, and suggests that it is commonly so closely

associated with the magnetite that it is not liberated during the crushing and magnetic separation of the ore.

Carbonaceous material

Carbonaceous material is present in minor amounts as very fine-grained dust (Figure 35) and opaque coatings in the slaty iron-formation. Gruner (1946, p. 21) indicated that it may be stylolitic. It appears opaque in the slaty iron-formation due to its proximity to dark minerals such as greenalite and stilpnomelane. It may be present in some of the chert of the cherty iron-formation, though its fine grain size makes it difficult to identify with certainty.

Evidence of organic activity during deposition of iron-formation is given by stromatolites. Preserved microbiotic assemblages of blue-green algae, which may or may not have been related to stromatolite deposition, have been identified in the Gunflint Iron Formation (Walter, 1976, p. 320; Condie et al, 2000). Some of the algae resemble present-day bacteria that grow in reducing conditions and precipitate ferric hydroxide (Evans, 1993, p. 255).

Limited carbonaceous material in the cherty members of the Biwabik Iron Formation may be expected as it has a lower specific gravity, and the carbonaceous material would be winnowed out during reworking. The reworked materials (i.e., cherty iron-formation with granules) would tend to contain less carbonaceous material than the slaty iron-formation (LaBerge, 1964).

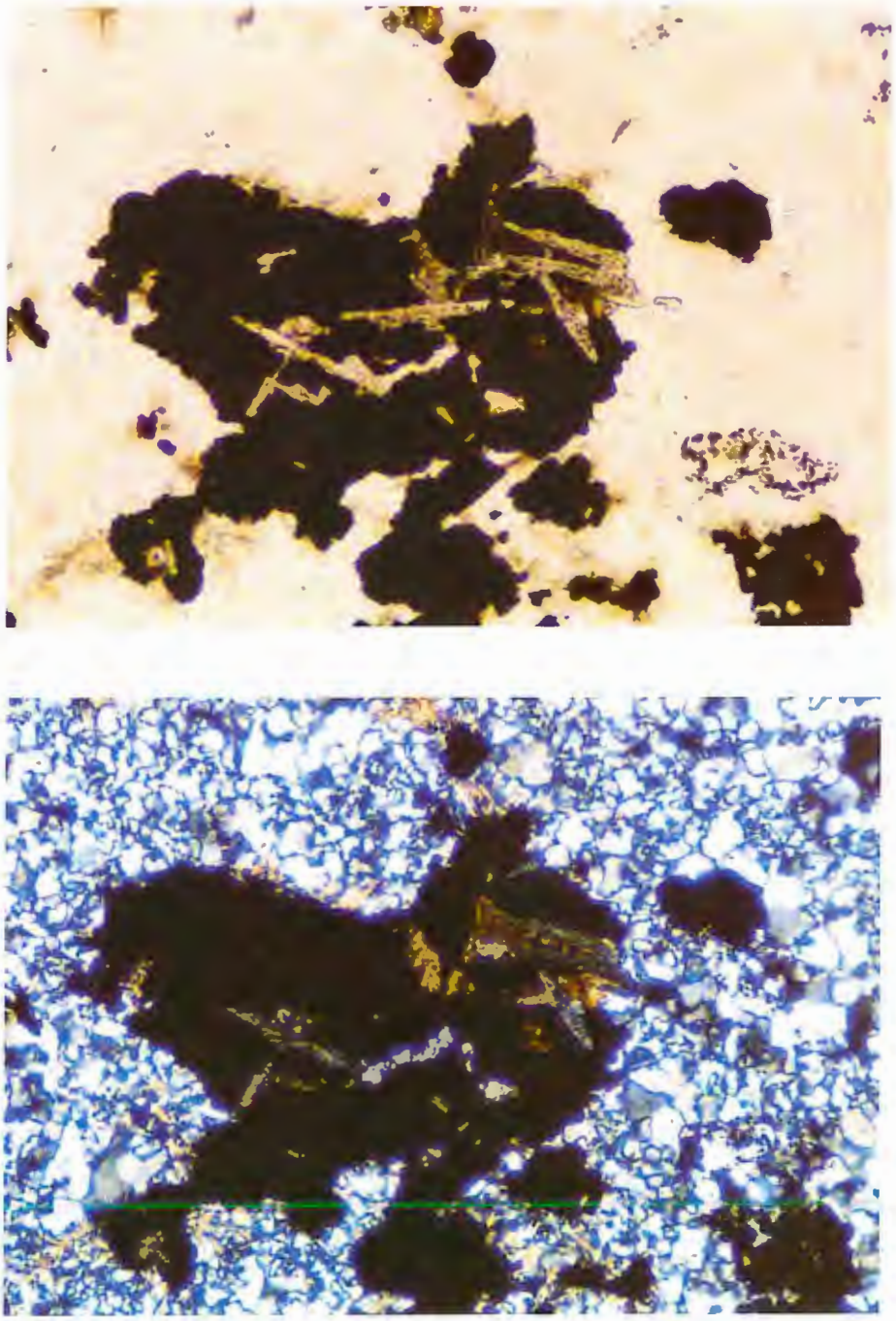

Figure 34. Apatite crystals surrounded by magnetite with minor carbonate. Chert cement. Note parallel extinction of center horizontal grain. Upper view plane light, lower view crossed polars. Field of view is 1.0 mm wide.

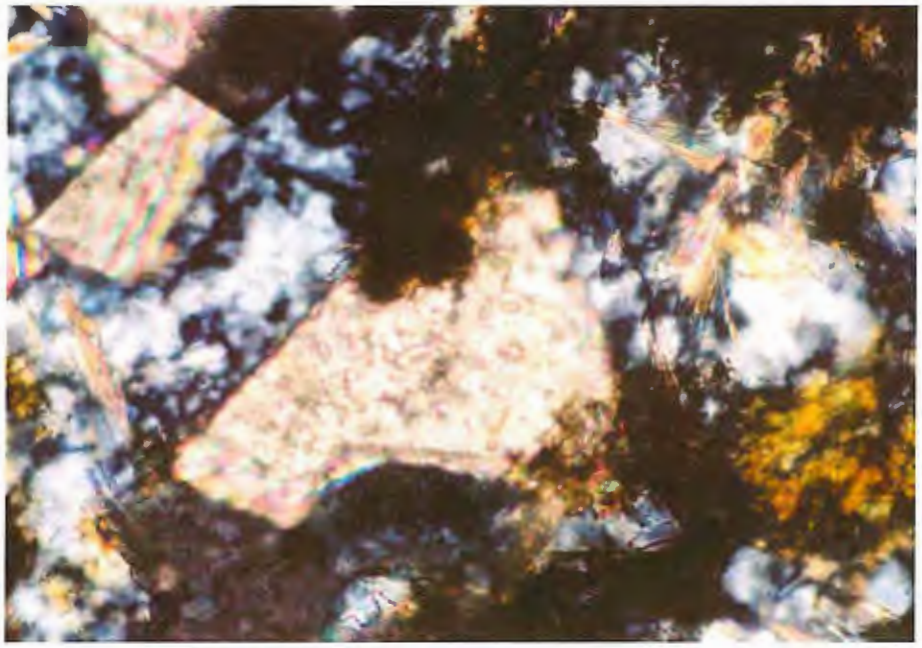

Figure 35. Black spheres of opaque material (possibly carbonaceous). Cement of chert replaced by coarse carbonate crystals and needles of minnesotaite. Crossed polars. Field of view is 0.25 mm wide.

Environment of Deposition:

Iron-formation of Precambrian age has been grouped into two types with different depositional features. Specifically, there is Algoman type, which consists of thin, varve-like bands and the granular Superior type, which is named for the iron-formations in the Lake Superior region. Morey and Southwick (1995) and Gole and Klein (1981) argued that these divisions do not imply different chemical processes in the formation of the two types of iron-formation. They presented similarities in bulk composition and mineral assemblages between the two, suggesting that the physical environment of deposition was all that distinguished the two types of iron-formation. Algoman type iron-formation may reflect deposition in an unstable basin, resulting in thinner formations with less lateral extent. Superior type iron-formation is representative of deposition in a stable basin where larger thicknesses and extents were deposited (Gole and Klein, 1981). Textural evidence suggests cherty iron-formation was deposited in shallow, tidal zones while the slaty iron-formation was simultaneously forming in deeper water (R. Ojakangas, 1983).

Most researchers agree that the earth's atmosphere was significantly different in Precambrian times. In 1927, MacGregor proposed that the deposition of iron-formations in the Precambrian was due to a higher CO_2 and a lower O_2 pressure in the atmosphere, which allowed iron to be soluble in the ferrous state (Lepp, 1975, p. 5). In 1955, Rankama proposed that the Precambrian atmosphere was mostly unoxygenated based on evidence from weathering of a Precambrian diorite. During the 1950s and 1960s, work by Tyler and Twenhofel, White, Lepp and Goldich, Cloud, and James supported the idea, and it gained general acceptance (Lepp and Goldich, 1964, p. 319). Also, scientists working on the origin of life independently came up with the conclusion that the Precambrian atmosphere was oxygen-poor (Lepp, 1975, p. 6).

Condie et al (2000) hypothesized that the CO_2-rich, warmer atmosphere may be due to a mantle superplume event. A large number of mantle plumes would create higher sea levels, in part evidenced by the large amount of marine sediments preserved from the time period, including banded iron-formation. Simonson and Hassler (1996) also suggested higher sea levels facilitated the deposition of banded iron-formation. Isley (1995) and Condie et al (2000) proposed that buoyant hydrothermal plumes enriched in iron and silica and depleted in oxygen traveled into the upper water column along the continental shelf, where silica and iron deposited as a precursor to banded iron-formation. Morey (1992) presented evidence for a volcanic component to the Biwabik Iron Formation, including an ash-fall tuff and major element analysis showing a positive correlation between TiO_2 and Al_2O_3, suggesting the stilpnomelane is titanium-bearing and therefore of volcanic origin.

LaBerge (1964) suspected that polymerization of fine-grained opaline silica formed layers that were re-worked by waves or currents, forming rounded particles. Textural evidence of the primary minerals siderite and greenalite indicate they, too, may have been deposited as layers that were reworked by currents to form granules.

The majority of chert from core 22L8 appears to be cement. Simonson (1987) suggested a steep geothermal gradient caused rapid precipitation of silica after deposition of the original mineral precursors at the exclusion of other minerals. Rapid silica cementation occurs beneath modern day hot springs and other areas with steep

geothermal gradients and the modern cements range from opaline silica to megaquartz. According to Simonson (1987), rapid silica cementation indicates that the original iron-formation sediments have been enriched in silica, and that the cemented iron minerals are compositionally similar to the primary material deposited.

The origin of magnetite in iron-formations is debated. Metamorphism has been credited for creating magnetite, although magnetite is found in unmetamorphosed iron-formation. In the virtually unmetamorphosed Gunflint Iron Formation, siderite and greenalite are the most abundant iron minerals. Goodwin (1975, p. 290) attributes most of the magnetite in the Gunflint Iron Formation to thermal metamorphism accompanying diabase intrusions, although portions of the magnetite-bearing zones appear to have no direct relationship to intrusions or other metamorphic events. The heat generated by the 1.1 Ga Keweenawan Midcontinent Rift System has been hypothesized to be responsible for transforming the previously non-magnetic Biwabik Iron Formation to magnetic taconite (Cannon, 1998), although evidence for metamorphism in the Virginia Horn area is refutable. James, Broderick, and Gruner indicate that high grade metamorphism, such as that caused in the eastern Mesabi Range by intrusion of the Duluth Complex, does not produce additional magnetite and the magnetite does not display much difference in grain-size, texture, or distribution (LaBerge, 1964).

Perry and Tan (1973) proposed a model for a metamorphic or diagenetic origin of magnetite based on carbon isotope variations. They postulated that much of the iron in iron-formation was precipitated as ferric-oxide-hydroxide simultaneously with a variable amount of organic matter. Primary hematite could be reduced to magnetite by the presence of organic carbon. This model provides an explanation for the coexistence of magnetite and hematite in many iron formations. The coexistence implies that the reaction stopped when the local system became depleted in carbon.

LaBerge (1964) indicated that magnetite appears to have been developed by the oxidation of pre-existing ferrous-iron minerals, such as siderite and greenalite. The presence of carbonaceous material prevented oxidation of ferrous iron. Therefore, layers that are carbon-rich (slaty iron-formation) are expected to contain little to no magnetite.

This fits observations of core 22L8 where the presence of magnetite appears independent of chert but dependent on iron carbonate and iron silicate.

Conclusions:

The Biwabik Iron Formation is a chemical precipitate with a predominant volcanic and/or hydrothermal source. The primary diagenetic or early forming minerals are chert (cement), greenalite, siderite and hematite. Carbonaceous material was deposited simultaneously. Secondary forming minerals are magnetite, minnesotaite, talc, clinochlore, ankerite, pyrite, and apatite. Cherty iron-formation formed on a shallow, tidally-influenced shelf, while slaty iron-formation formed in deeper water. Deposition probably occurred during the transition of a non-oxygenated atmosphere to an oxygenated atmosphere. Magnetite seems to have formed in the presence of oxygen.

Recommendations:

Textures in the slaty iron formation were difficult to observe under transmitted light. Electron microscope study of the slaty layers might indicate depositional features that are otherwise hidden by the dark fine-grained minerals and carbonaceous material. Lack of carbonaceous material may be linked to magnetite formation, and therefore further study of the carbon-rich sections may provide additional clues about original iron minerals. The spherical structures within chert and greenalite are seemingly unique features in iron-formation that warrant further investigation under high-powered magnification.

Part II. Joint Orientation

Studies to determine the general joint orientation in the Biwabik Iron Formation have been conducted (Gruner 1946; White 1954, p. 56), but mine-specific joint orientation studies have not been published. A mine-specific joint measurement study was conducted in the Virginia Horn area to possibly benefit mine planning and to attempt to determine the relative age of the jointing with respect to the major structural events that occurred in the region. Measurements were made in the EVTAC North, South, and Spruce pits; the MINNTAC East and West pits; and the Ispat Inland Minorca and Laurentian pits.

Methods for joint measurement and analysis:

Due to the high concentration of magnetite in the Biwabik Iron Formation in the Virginia Horn area, a magnetic compass was not used to measure strikes of joints. A Global Positioning System (GPS) unit and a sun compass were used to determine the strikes. GPS proved to be cumbersome and required a large length of fracture on footwall exposures on pit floors in order to make measurements. The sun compass was portable and did not require large outcrops for accurate measuring. Therefore, the majority of joint measurements represent sun compass data. The sun compass looks much like a sundial in that it has markings in five-minute intervals for the time of day around its perimeter. Aligning the shadow of a string stretching across the middle of the sun compass with the appropriate time marking on the perimeter orients the compass to north-south. A protractor is used to determine the number of degrees that a joint differs from north-south on the sun compass. Strike measurements made with the sun compass were rounded to the nearest five degrees.

Dip was measured using the clinometer of a Brunton compass. Dips along pit walls were sighted from a distance, and dips along pit floors were measured with the compass edge placed directly on a flat object aligned with the dip surface. As pit floors were generally level, there was little exposure of joints in three dimensions along the pit floor. The majority of dip measurements were taken along pit walls. Pit walls were inspected prior to measuring joints to determine whether rocks were in place, or if rocks

had slumped. Slumping was identified by the juxtaposition of blocks of rock, the wide variation in joint direction, and the uneven level of the top surface of the pitwall with the horizon. The explosive blasts used to dislodge the rock in the pit commonly cause slumping of rock in the pit wall, especially in slaty iron-formation. Joints in slumped rock were not measured. Therefore, there are few dip measurements available in the data set. Joint measurements are presented in tables in Appendix IV.

Rose diagrams were produced with RockWare Utilities software. Strikes in azimuth notation were used to produce mine-specific rose diagrams as well as a compilation rose diagram including all data from the mine-specific measurements. Visual inspection of the rose diagrams shows the main strike directions. Statistical analysis performed in the Rockware program provides a measure of dispersion (R-mag) standardized between zero and one. Data sets with a large dispersion will have Rmag values near zero, those with little dispersion will have Rmag values near one (Davis, 1986, p.319). In addition, the program calculated the maximum percentage of measurements presented by a filled sector, or petal, in the sample interval.

Results of joint analysis:

A total of 309 strike and 31 dip measurements were made in the mine-specific studies. In addition, 263 joint measurements taken for a structural study by Mark Jirsa and Terry Boerboom of the Minnesota Geological Survey were provided for rocks within and near the Mesabi Range (Virginia Horn area). Jirsa and Boerboom's measurements were broken out based on rock age, and eight measurements were available for the iron-formation and Pokegama quartzite. Two-hundred fifty-seven joint measurements were available for Archean rocks.

From White's (1954, p. 56) rose diagram of 290 joint strike measurements between Mesaba and Coleraine (most taken by Gruner, 1946), the following was noted:

"The three main joint sets strike about N10E, N45W, and N80W. Joint planes are commonly straight, long, and essentially vertical, the dips being steeper than 70 degrees. At any one place, two of the joint sets are generally more prominent than the third."

In azimuth notation, the main directions noted in Gruner and White's study were 10°, 315°, and 280°. The compilation of Jirsa and Boerboom's joint measurements in Archean rocks showed the following main directions: 40°, 350°, and 280°. The Rmag value of 0.08 indicates dispersion is large in the Archean rock joint measurements. The maximum percentage presented by a petal was eight. Eight joint measurements were made by Jirsa and Boerboom within the Biwabik Iron Formation and the Pokegama Quartzite, with directions of 10°, 35°, 40°, 85°, 280°, 335°, 340° and 15°. All dips were vertical. Appendix V contains rose diagrams for the Jirsa/Boerboom study, as well as the mine-specific studies listed below. Rose diagrams were used to find the joint directions that occurred most frequently. Field observations indicated that the most prominent joint direction (i.e., joints with the most length and width) often differed from station to station.

EVTAC North

A total of 111 joint strike measurements were taken from 13 stations in the EVTAC North pit. Dominant joint directions were 290°, 340°, and 30°. These measurements are shifted 10° east and 10° west from the main directions found in Jirsa and Boerboom's study of Archean rocks. The data from the EVTAC North pit showed a high dispersion (Rmag value of 0.16). The maximum percentage represented by a petal was 11.7.

EVTAC South

A total of 16 joint strike measurements were taken from seven stations in the EVTAC South pit. Dominant joint directions were 280°, 320°, 10°, and 60°. The 280° measurement is consistent with the Gruner/White and Jirsa/Boerboom studies. Ten degrees and 320° match or are near Gruner's measurement findings. The EVTAC South pit displays the highest dispersion of all mines studied with an Rmag value of 0.04. The maximum percentage represented by a petal was 12.5.

EVTAC Spruce

A total of 10 joint strike measurements were made from four stations in the EVTAC Spruce pit. Main directions were 310° and 40°. The 310° measurement is consistent with the Gruner/White and Jirsa/Boerboom studies, 40° matches results of the Jirsa/Bourboom study. Dispersion was high, but relatively low compared to the other pits with an Rmag value of 0.21. The maximum percentage represented by a petal was 30.

MINNTAC East

A total of nine joint direction measurements were made at four stations in the MINNTAC East pit. The rose diagram shows 280° as the dominant direction. The Gruner/White and Jirsa/Boerboom studies also found 280° as a dominant direction. The MINNTAC East pit displayed the lowest dispersion of all of the mines, with an Rmag value of 0.31. The maximum percentage represented by a single petal was 22.2.

MINNTAC West

A total of 17 joint direction measurements were made at six stations in the MINNTAC West pit. Dominant joint directions were 325°, 50°, and 90°. These directions are 10° from measurements made in the Gruner/White and Jirsa/Boerboom studies. Dispersion was high, with an Rmag value of 0.19. The maximum percentage presented by a single petal was 17.6.

Ispat Inland Minorca

A total of 93 joint measurements were made at nine stations in the Ispat Inland Minorca pit. Main directions were 320° and 30°. These are close to the 315° and 40° values found in the Gruner/White and Jirsa/Boerboom studies, respectively. Dispersion was high, but relatively low compared to other pits, with Rmag at 0.23. The maximum percentage presented by a single petal was 19.4.

Ispat Inland Laurentian

A total of 43 joint direction measurements were taken from five stations in the Laurentian pit. Main directions were 310° and 30°. These are close to the 315° and 40° directions in the Gruner/White and Jirsa/Boerboom studies, respectively. The Rmag value of 0.11 indicates large dispersion. The maximum percentage presented by a single petal was 16.3.

Summary and Discussion:

In a rose diagram of combined results from of all seven of the pit-specific studies (299 measurements), the main directions were 310° and 30°. Dispersion in the entire data set was large (Rmag of 0.03). The maximum percentage represented by a single petal was 12.7.

Table 1 shows the dominant joint directions found in each study. Directions found in two or more studies include: 10°/190°, 30°/210°, 40°/220°, 100°/280°, 130°/310°, and 140°/320°. The most common direction, shared as a dominant direction in four studies, was 280°.

The Rmag values were high in each of the mine-specific studies, indicating large dispersion of joint orientation in general. The amount of dispersion from largest to smallest for joints measured at the individual mine pits are: EVTAC South, Ispat Inland Laurentian, EVTAC North, MINNTAC West, EVTAC Spruce, Ispat Inland Minorca, and MINNTAC East. While the greatest variety of joint strike orientation is found near the inflection point of the Virginia Horn syncline (EVTAC South Pit), joints in the Ispat Inland Laurentian and MINNTAC West Pits (located where the iron-formation structure appears less complex on a large scale) display a larger dispersion than the Minorca mine located at the inflection point of the Virginia Horn anticline. Neither the smallest nor largest data sets contain the highest variation in fracture orientation, suggesting that the size of the data set does not correlate with the amount of variation in fracture orientation.

Upon visual inspection of the rose diagrams in the approximate locations within the Biwabik Iron Formation (Figure 35), there is no apparent pattern in the major joint direction with regard to the strike of the iron-formation. The complexity of the joint

Table 1

Dominant Fracture Directions

Direction	Jirsa/Boerboom Archean	Gruner/White	EVTAC North	EVTAC South	EVTAC Spruce	MINNTAC East	MINNTAC West	Ispat Inland Minorca	Ispat Inland Laurentian
10/190		X		X					
15/195									
30/210			X					X	X
35/215									
40/220	X				X				
50/230							X		
60/240				X					
85/265									
90/270							X		
100/280	X	X		X		X			
110/290			X						
130/310					X				X
135/315		X							
140/320				X				X	
145/325							X		
155/335									
160/340			X						
170/350	X								

X denotes the direction was dominant in the study.

patterns is not clearly related to the location of a mine within the large-scale Virginia Horn structure. Smaller-scale features such as minor folds and faults, or large-scale features such as the underlying bedrock structure may have greater control over mine joint orientations than the syncline-anticline structure of the Virginia Horn. This may indicate that joint formation is locally complex, dependent on more than the macrostructure of the area.

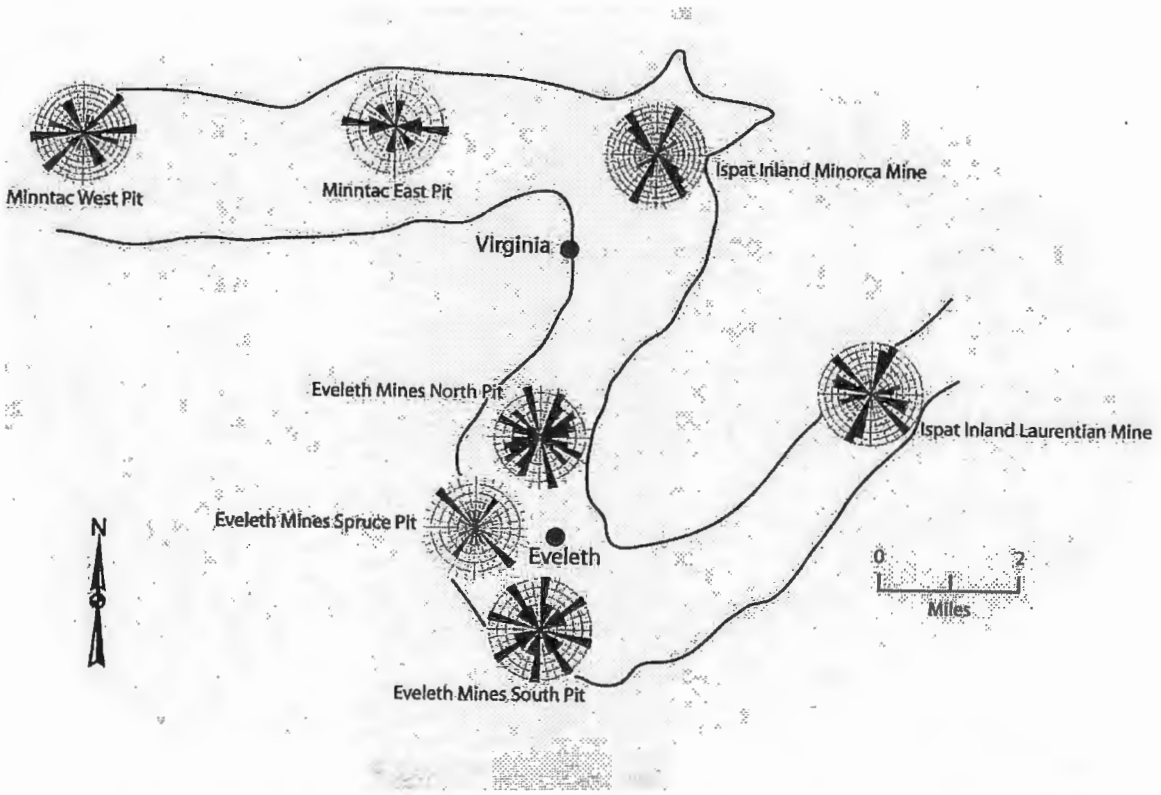

Figure 36. Biwabik Iron Formation joint strikes in the Virginia Horn area.

Hatcher (1995, p. 257) noted that if an unmineralized joint set cuts a mineralized joint set, the unmineralized set either formed later than the mineralized set, or was subject to stress that kept it closed to fluid circulation. Mineralization was noted in several joints measured in the mine pits. In the MINNTAC West pit, joints striking 280° commonly have a characteristic amethyst/ankerite coating. The EVTAC North pit also displayed quartz and carbonate mineralization on joints striking 280°, but several other joint

directions were inconsistently mineralized. Pyrite was noted from field observation in one joint at the EVTAC North pit. Quartz and carbonate mineralization along joints was noted in the EVTAC Spruce and South pits, and in the Ispat Inland Minorca pit. Cross-cutting relationships of various joints in the Biwabik Iron Formation are ambiguous. For example, in the area of the EVTAC North pit, joints striking 25° appear to terminate at the intersection of joints striking 305°. Within feet of these joints, the opposite relationship was found. Mineralization along joint planes may have allowed stresses to resolve across a joint surface where otherwise they would have been arrested. Mineralization and subsequent removal of mineralization may account for some of the inconsistencies with cross-cutting relationships, or the joints may be of the same age, belonging to the same tectonic episode (Pollard and Aydin, 1988). The age relationship of the joint directions is not clear from the limited observations of mineralization along the fracture planes.

Out of a total of 31 dip measurements made in the mine-specific study, dips of the fractures in the iron-formation vary from 78° to vertical. Dip amount is not consistent among fractures propagating in the same direction. For example, at one station the joints striking 280° were vertical, and at another station in the same pit the joints striking at 280° were dipping at 81°. Dips of joints in the Archean rocks vary between 10° and vertical, but the majority of the joints are between 70° and vertical. Dips in the Jirsa/Boerboom measurements of Pokegama Quartzite or iron-formation joints were vertical.

Bedding-parallel joints are also found in the iron-formation. Slickensides were observed along many of these surfaces and indicate movement and the presence of fluid along these planes. Slickensides were most common near the upper cherty/lower slaty contact. Mineralization on the slickenside plane (based on field observation) consisted of epidote, chlorite, quartz, and carbonates. Measurements were made of the striation direction on slickensides found in-place, although the quantity of measurements was few. While there are not enough slickenside measurements to accurately determine horizontal movement directions in the iron-formation, the presence of slickensides does indicate horizontal displacement. Two measurements of slickensides were made in the EVTAC

North pit (70°/250 and 140/310°) and one measurement was made in the EVTAC South pit (25°/105°). Four measurements of slickensides were made in the Ispat Inland Minorca pit (10°/190°, 140°/320°, 145°/325°, and 150°/330°).

Stresses that may have caused jointing in the Biwabik Iron Formation of the Virginia Horn area include stress fields in place during major tectonic events and the stress of loading or unloading (during glacial advance or retreat). Tectonic fractures form at depth in response to abnormal fluid pressure and may form at depths less than 3 km. Unloading joints form at depths of 200 to 500 m as erosion removes overburden, and thermal-elastic contraction occurs. Contemporary tectonic or remaining ancient stresses may serve to orient these joints. Release of horizontal stress provides a similar opportunity for release joints to form. The existing rock fabric controls orientation of release joints. Release joints form late in the history of an area and are ultimately oriented perpendicular to the original tectonic compression that formed the dominant fabric in the rock (Pollard and Aydin, 1988).

Two tectonic events have affected the structure of Early Proterozoic rocks in Minnesota. The Penokean orogeny (approximately 1.85 Ga) caused folding and metamorphism of the rocks. The rocks of the Mesabi Range were moderately affected (Morey, 1970) and many structures in the Mesabi Range have trends consistent with development during the Penokean orogeny (Morey, 1970). The Lake Superior syncline formed in the Middle Proterozoic (1.1 Ga). As a consequence, the Mesabi range dips gently south. Gruner (1946) and White (1954, p. 67) concluded that the joint system in the Mesabi Range is consistent with, but not necessarily related to, the Lake Superior syncline. The axis of the Virginia Horn anticline/syncline is parallel to the axis of the Lake Superior syncline. White (1956, p. 67) indicated that assuming a northwest-southeast compression, joints striking 10° and 280° would be shear fractures, and those at 315° would be extension fractures forming perpendicular to the compression.

A number of faults exist in the Virginia Horn area of the Biwabik Iron Formation. Morey (1970, p. 202) noted that faults commonly strike 285° or 340° with displacements of less than 15 m. Fractures may propagate from older crystalline basement rocks to overlying unfractured sedimentary rocks (Hatcher 1995, p.143). Morey (1970) noted that

faults that cut the iron-formation are thought to represent rejuvenated movements on older structures that developed initially in the Archean. Joints frequently form adjacent to brittle faults. Movement along faults commonly produces a series of systematic fractures in which spacing decreases closer to the fault zone, and the number of sets also increases (Hatcher, 1995, p. 145).

Joints are most effectively initiated in the presence of fluid, and form at preexisting flaws in the rock. In general, fluid pressure must exceed the least compressive stress for a fracture to develop, indicating that the initial joint surface is approximately perpendicular to the least compressive stress. In anisotropic rock, planes of weakness may be favored for jointing even if they are not perpendicular to the least compressive stress (Pollard and Aydin, 1988). Bedding and foliation planes in coarse-grained rocks or sections of alternating sedimentary rock types may be barriers to joint propagation due to differences in stress magnitude between layers (Pollard and Aydin, 1988). Variation in bed thickness may also affect propagation direction. Therefore, it is possible that fractures in cherty iron-formation may not propagate through, or may change direction when propagating through, slaty iron-formation and vice versa.

Conclusions:

There are common joint orientations in the Biwabik Iron Formation near the Virginia Horn area. The joints do not appear to vary with the strike of the iron-formation in the anticline/syncline structure of the Virginia Horn. A dominant joint direction found in Archean rocks of the Virginia Horn area (280°) is close to the dominant fault strike direction (285°) in the Virginia Horn. Dominant joints strike between 280° and 290° were found in three of the eight mine pits surveyed, suggesting some control by underlying Archean basement rocks.

Recommendations:

Detailed study of systematic fractures provides information about the principal stress directions involved in brittle deformation. Details such as feather or chevron patterns, hackles, and fringe structures that may be used to determine fracture

propagation direction, mode of fracture, and the stress state for the history of the joint propagation were not closely observed in this fracture orientation study. It is recommended that more detailed information be collected to allow for an analysis of the age of fractures within the Biwabik Iron Formation.

Appendix I – Photomicrograph Information

Figure	Unit	Core #	Footage
6	Lower Upper Cherty	8971	233
7	Lower Upper Cherty (lean zone)	8971	227.5
11	Top of Lower Cherty (waste)	22L8	111
12	Top of Lower Cherty (ore)	22L8	185
13	Top of Lower Cherty (pink)	22L8	149
14	Top of Lower Cherty (waste)	22L8	122
15	Top of Lower Cherty (ore)	22L8	135
16	Footwall Taconite	22L8	320
17	Lower Slaty (waste)	22L8	78
18	Top of Lower Cherty (ore)	22L8	160
19	Top of Lower Cherty (ore)	22L8	185
20	Top of Lower Cherty (ore)	22L8	160
21	Bottom Lower Cherty	5697	432
22	Top of Lower Cherty (waste)	22L8	185
23	Top of Lower Cherty	5697	328
24	Lower Slaty (waste)	22L8	103
25	Top of Lower Cherty (ore)	22L8	135
26	Top of Lower Cherty (ore)	22L8	170
27	Top of Lower Cherty (ore)	22L8	161
28	Bottom of Lower Cherty (ore)	22L8	210
29	Top of Lower Cherty (ore)	22L8	185
30	Top of Lower Cherty (ore)	22L8	185
31	Top of Lower Cherty (ore)	22L8	175.5
32	Footwall Taconite	22L8	292.5
33	Bottom of Lower Cherty (ore)	22L8	210
34	Top of Lower Cherty (pink)	22L8	149
35	Lower Slaty (waste)	22L8	75

Note: Thin sections from cores 8971 and 5697 (provided courtesy of EVTAC) were observed for background information, but were not logged.

Appendix II – Observations for core 22L8

Feet 20-62: The Lower Upper Cherty is banded, fine-grained, dark grey in color with magnetite-rich layers and coarser grained white to grey-green silica layers. It has oxidized to an orange color. Silicate-rich layers contain dark specks. Predominantly fine-grained dark green chert with elongate dark grains (granules). Magnetism concentrated in layers, though individual magnetite grains not always visible with naked eye. Wavy laminations with coarser grained layers and lenses which pinch in and out. Possible cross-bedding. Decreasing magnetite with depth. Thin section examination reveals feet 20-62 to contain siderite, stilpnomelane, greenalite, and minnesotaite. Layered: carbonate-rich with minor tiny magnetite crystals and iron-silicate-rich with granules and larger magnetite crystals than in carbonate layer. Carbonate is both in spherical clusters of crystals and coarse-grained. Chert and minnesotaite bands interrupt the carbonate layers. Minnesotaite is replacing chert. Chert is both clear and cloudy brown. Chert tends to be finer grained where replacing granules. There are minor chert veins. Carbonate definitely concentrated in layers and not intermixed with chert layers. Carbonate seems to be replaced by magnetite. Chert is mixed in with iron-silicate layers.

Feet 62-109: The Lower Slaty is non-magnetic with partings. It is dark-grey; fine-grained except for occasional small (1 to 5 cm wide by 0.5 to 1 cm high), coarser grained white pods. Pitting occurs around these pods. May be slightly oxidized, mainly along fractures. Few narrow (1-3 mm) quartz veins and similar pyrite veins. Larger, more coarse-grained pods are up to 10 cm wide. Some disseminated pyrite grains, some wavy laminae. Even in the most finely laminated black, slaty material, there are small pods of coarser grained silica (which is white weathered, black fresh). Some slickensides along laminations/partings and pyrite is associated with these. Core is quite broken up along partings in some areas. Appears to be an abrupt grain size change from pods to surrounding grains rather than gradational. Coarser grains appear rounded, but not spherical and are moderately varied in size. Toward the base of the unit, larger, more coarse-grained pods contain clasts of the finer grained slaty material. At base of this layer, there are large chert nodules and thicker quartz veins. Microscope study reveals

that the Lower Slaty contains chert, siderite, minnesotaite, stilpnomelane, and greenalite. The minerals are intermixed and ribbons of stilpnomelane or other minerals define wavy, discontinuous layers. The main mineral layers are composed of green, wavy layered iron-silicate. Layer thickness varies between 0.1 cm to 1.5 cm thick. They are extremely fine-grained and very dark; isotropic under crossed polars. Reddish brown blebs occur at the interface between stilpnomelane and siderite. Chert exists as scarce, small, isolated crystals admixed with the iron silicate layer, and is being replaced by radiating minnesotaite crystals. Lenses (up to 1 cm high) within the slaty layers contain granules, and the granules grade out and become increasingly elongate toward the ends of the lens, stretching out to form a layer. It is unclear whether these lenses are clasts, better-cemented material, or representative of further replacement/reaction. The lenses are mainly carbonate and minnesotaite with minor chert. Chert is both clear and brownish. Granules are mainly siderite or radiating sheaves of minnesotaite. It is difficult to tell if there are volcanic shards present. Siderite is fuzzy and spherical in habit and is being replaced by minnesotaite; some siderite is more coarsely crystalline. The coarser crystals appear around the edge of the more ill-defined crystals and appear to be recrystallizing from the fuzzy mass. Minnesotaite grows at the interface between siderite and chert. The fuzzy siderite appears to be replacing chert. Unidentified opaque areas are probably rich in carbonaceous material. Stilpnomelane is present in a needly habit as well as in wavy, thin layers. Greenalite is nearly opaque and associated with stilpnomelane and siderite. Siderite is found in granular shapes in the pods as well as in wavy, discontinuous layers associated with stilpnomelane and greenalite. Chert becomes more abundant near the bottom of the Lower Slaty, both as 0.5 mm thick veins and in the layers. A chert-rich, granular layer in the lower slaty has desiccation cracks in the granules and many are squished. Minnesotaite is the dominant mineral in the granular layers at the base of the Lower Slaty, and it is replacing chert. There is black material and black powder in many of the granules which may be magnetite or organic material. Greenalite appears to be altering to or replaced by stilpnomelane, stilpnomelane needles grow out of greenalite. Greenalite tends to be in rounded clumps, and there is more of it with siderite than with stilpnomelane. Near base of the Lower Slaty, magnetite octahedra

have formed in a chert/siderite rich layer. Stilpnomelane takes on a more fibrous nature and may actually be chlorite.

Feet 109-130: The Lower Cherty waste zone is non-magnetic at the top with increasing magnetite content toward the bottom. The very top of this zone contains clear chert nodules. The non-magnetic section of core is greenish grey to black in color with gradations between fine- and coarse-grained layers. Pyrite is disseminated in the fine-grained layers. Where the core has partings, there are shiny slip surfaces with coatings of pyrite. Quartz veins are common in this layer. Hematite is in wavy layers, and large irregularly shaped pieces of jasper are found in layers of coarse-grained green silicate matrix. Layers of very fine-grained greenish-black iron silicate are interspersed. As the core becomes magnetic, dark concentrated magnetite layers form sharp contacts with the surrounding silicate, and the core takes on a more banded appearance, with discrete boundaries between finer and coarser grained material. Microscopic examination reveals the granular texture of the top of the lower cherty waste-zone. Chert and minnesotaite are the dominant minerals in the non-magnetic part of the core. Chert exists as granules and interstitial to the granules, and the granules are being replaced by minnesotaite. In places, the chert granules are almost completely obliterated (i.e., replaced) by minnesotaite. The chert is mostly clear, but there are brownish blotches defining parts of some granules. Greenalite, stilpnomelane, ankerite, and magnetite were also identified in this zone by means of x-ray diffraction. Minnesotaite exists as radiating aggregates replacing chert, and nucleating on magnetite. Ankerite is found replacing granules of chert or greenalite, often associated with magnetite which is also replacing greenalite granules. The ankerite may be in rhombs or as spherical blebs of crystals. Stilpnomelane is fibrous in habit and found as granules. Chert, minnesotaite, and possibly stilpnomelane replace greenalite. Chert is replacing platy minnesotaite and radiating minnesotaite is replacing chert in the same granule. Carbonate is also replacing chert. Magnetite is closely associated with iron-silicates and carbonate, less so with chert. It is disseminated as octahedra as well as blebby in a network. Some veins of magnetite are associated with carbonate.

Feet 130 to 203: The top portion of the Lower Cherty ore zone has three subzones. Subzone 130 to 141 is greenish-white to gray on the weathered surface, green to black on the fresh surface. It is distinguished by wavy, uneven bedding of chert, iron silicate, and magnetite. There are numerous bedding parallel fractures with shiny, black slip-planes along partings and pyrite mineralization. Magnetite is present in concentrated bands and disseminated within the silicate matrix. Magnetite bands become thicker down-section (up to 3 cm thick). Subzone 142-145 is classified as the top of the Lower Cherty pink ore. As the name would suggest, there are pink layers among the dark grey layers. This is a massive unit of taconite with irregular clasts of carbonate and chert and mottlings of magnetite. Magnetite is concentrated around the carbonate clasts. Subzone 146-203 is dark grey on the fresh surface, but oxidation gives it a light grey to white color. The surface is quite pitted, with mm-sized pits that are closely spaced and 10-mm sized pits that are more widely spaced. Pits become more lens-shaped downsection. At foot 160, there are stylolites. Bands become blotchy, and silicate- and magnetite-rich blebs appear. White 2 mm thick veins with fibrous white minerals growing in fractures appear at 183 feet. These continue down the length of the core, about 1 every two feet. Discrete mixtures of more silicate-rich, carbonate-rich, and magnetite-rich areas are both banded and in breccia-like clasts. In thin-section, this ore is granular with different sized granules in discrete laminae, sometimes graded. There is chert, greenalite, siderite, minnesotaite, and magnetite. Chert is coarse-grained to very fine-grained. It is interstitial between greenalite granules and is also replacing greenalite granules. Some granules appear to be made of very fine-grained chert mixed with fibrous minnesotaite. Some of the chert is brown in plane light, and has a yellow tinge under crossed-polars suggesting the presence of fine-grained impurities (carbonaceous material or hematite dust?). Chert has been replaced by minnesotaite, but chert also replaces minnesotaite and carbonate. This suggests two generations of minnesotaite. Siderite is coarse grained, replacing greenalite granules and being replaced by minnesotaite, yet it also exists in small spherical crystals mixed in with minnesotaite. Ankerite is crystalline and fine-grained. Some optically continuous crystals are granule-shaped, suggesting ankerite has replaced greenalite. Granular crystalline ankerite is closely associated with magnetite and replaces quartz. In one case, carbonate forms a circular structure around magnetite.

Carbonate has a browner color at the magnetite/carbonate interface. Minnesotaite in radiating crystals has replaced chert and greenalite, but is also in a platy habit associated with greenalite. Magnetite has replaced the finer grained minnesotaite, while blady crystals nucleate at the edge of magnetite, finer minnesotaite, and chert. Greenalite is brownish-green and is composed of tiny spherical shapes. It is almost isotropic with opaque blebs and wavy layers in it. Are these carbon-rich or magnetite-dust rich? Chert, minnesotaite, and carbonate replace greenalite. Magnetite forms a rim around granule shapes and partially replaces granules of greenalite. It is closely associated with carbonate and minnesotaite. In some cases, magnetite around the edge of a greenalite granule appears to have preserved the greenalite from being replaced. Magnetite is in lensoid crystals or blocky crystals. Apatite crystals may occur at the boundaries between magnetite and chert; the crystals are blady and have pitted surface texture. Granules disappear for intervals and then return.

Feet 203-242 is the bottom Lower Cherty ore zone. It is moderate to strongly magnetic and slightly oxidized in parts. Magnetite is in black bands between layers of greenish gray to white (weathered) iron silicate- and chert-rich layers with black magnetite grains disseminated throughout. A white fibrous mineral forms 2 mm thick layer-parallel veins. Occasional pieces of carbonate with magnetite rims surrounding them are in the iron silicate- and chert-rich layers. In some cases, carbonate blobs are almost completely replaced by magnetite. Some red hematite-colored layers between magnetite bands. Pyrite vein (0.5 cm thick) at foot 223. Thin sections of the bottom Lower Cherty ore zone show it is composed of the minerals chert, ankerite, magnetite, pyrite, and minnesotaite. It is granular, with desiccation cracks in some of the chert and minnesotaite granules. Minnesotaite is brown to yellow pleochroic, and fibrous as well as in platy crystals resembling greenalite. Magnetite exists as partial replacement of chert and minnesotaite granules. Chert is interstitial as well as in granules. It is associated with minnesotaite. Chert is replaced by and replaces carbonate. The chert-granule-rich area is mostly magnetite-free. Chert is mixed with minnesotaite in some granules. Pyrite is associated with fine-grained carbonate. Carbonate is both coarsely crystalline and fine-grained. Ankerite is associated with magnetite; crystals seem to be fuzzy on edges

without sharp crystal edges. Minnesotaite is actually talc on x-ray diffractograms. It is extremely fine-grained and mostly has a platy habit. It is replaced by quartz. It is found interstitially as radiating crystals, but is platy in granules. There are zones of circular concentrations of carbonate surrounding magnetite.

Feet 243-249 constitute the bottom Lower Cherty/footwall transition zone. Moderately magnetic, pale grey to dark greenish grey (fresh) to white weathered, with black, wavy magnetite layers 1 mm-4 cm thick. Thinly bedded. Disseminated magnetite is less concentrated as above and in some cases almost absent. The white fibrous veins are still present. Black, "graphitic" bedding-parallel slip-planes. 5 mm thick quartz veins parallel to and normal to bedding. Thin section examination shows this zone to be granular, with granules of fine-grained chert and very fine-grained minnesotaite or talc. Minnesotaite occurs as granule remnants. Magnetite is associated with iron-silicate and carbonate. Granules have desiccation cracks. Carbonate is associated with the platy, fine-grained minnesotaite and magnetite-rich areas. Chert replaces carbonate, carbonate replaces chert. Magnetite replaces iron silicate, chert replaces iron silicate, iron silicate replaces chert.

Feet 249-266: The footwall ore is moderately to strongly magnetic. It is dark grey to greenish grey (weathering white) thin bedded cherty magnetite taconite with black specks of disseminated magnetite, more concentrated than in the transition zone. There are black magnetite layers 1 mm to 5 cm thick (average 1 cm). White, fibrous bedding-parallel veins (talc?) less than 1 mm thick cut through the magnetite-rich layers. Red chert granules are found in the cherty layers. Magnetite rims surround reddish carbonate chips. Reddish, hematite-rich layers are found between the magnetite layers. Minor stromatolite fragments cross-cut layers. In thin section, this ore is granular, with the chert and iron-silicate granules aligned and flattened. Chert, minnesotaite, magnetite, hematite, and ankerite are present.

Feet 266-331: Footwall taconite is moderately to weakly magnetic, with magnetism decreasing down-hole. It is light to dark grey (white with dark specks and dark with

white specks on the weathered surface) very fine-grained silicate layered with sub-parallel slightly wavy magnetite-rich layers. Occasional jasper lenses and fragments and disseminated jasper granules. Red jasper granules increase down-hole, lending a slight pinkish tinge to the grey. Beds of green iron-silicate and hematite-rich layers increase down-hole. The last few feet of the hole are less regularly banded and more broken up/mixed together. Thin sections show chert, ankerite, minnesotaite, magnetite, and hematite.

Appendix III

Thin Section (Core # -- Feet below ground surface)	Stratigraphic Location
22L8—20.5	Lower Upper Cherty/Lower Slaty
22L8—43	Lower Upper Cherty/Lower Slaty
22L8—53	Lower Upper Cherty/Lower Slaty
22L8—64	Lower Slaty Waste
22L8—65	Lower Slaty Waste
22L8—75	Lower Slaty Waste
22L8—78	Lower Slaty Waste
22L8—91	Lower Slaty Waste
22L8—102	Lower Slaty Waste
22L8—103	Lower Slaty Waste
22L8—106	Lower Slaty Waste
22L8—108	Lower Slaty Waste
22L8—109	Top of Lower Cherty Waste
22L8—111	Top of Lower Cherty Waste
22L8—122	Top of Lower Cherty Waste
22L8—129	Top of Lower Cherty Waste
22L8—135	Top of Lower Cherty Ore
22L8—135.3	Top of Lower Cherty Ore
22L8—144	Top of Lower Cherty Pink
22L8—147	Top of Lower Cherty Pink
22L8—149	Top of Lower Cherty Pink
22L8—155	Top of Lower Cherty Ore
22L8—160	Top of Lower Cherty Ore
22L8—161	Top of Lower Cherty Ore
22L8—170	Top of Lower Cherty Ore
22L8—175.5	Top of Lower Cherty Ore
22L8—185	Top of Lower Cherty Ore
22L8—202	Top of Lower Cherty Ore
22L8—210	Bottom of Lower Cherty Ore
22L8—216	Bottom of Lower Cherty Ore
22L8—228	Bottom of Lower Cherty Ore
22L8—258	Footwall Ore
22L8—258.5	Footwall Ore
22L8—261	Footwall Ore

22L8—292.5	Footwall
22L8—307.5	Footwall
22L8—311	Footwall
22L8—320	Footwall
22L8—326	Footwall

Note: Thin sections photocopied on the following pages may show black circles. These were drawn with pen on the actual thin section during observation and are not a feature of the rock.

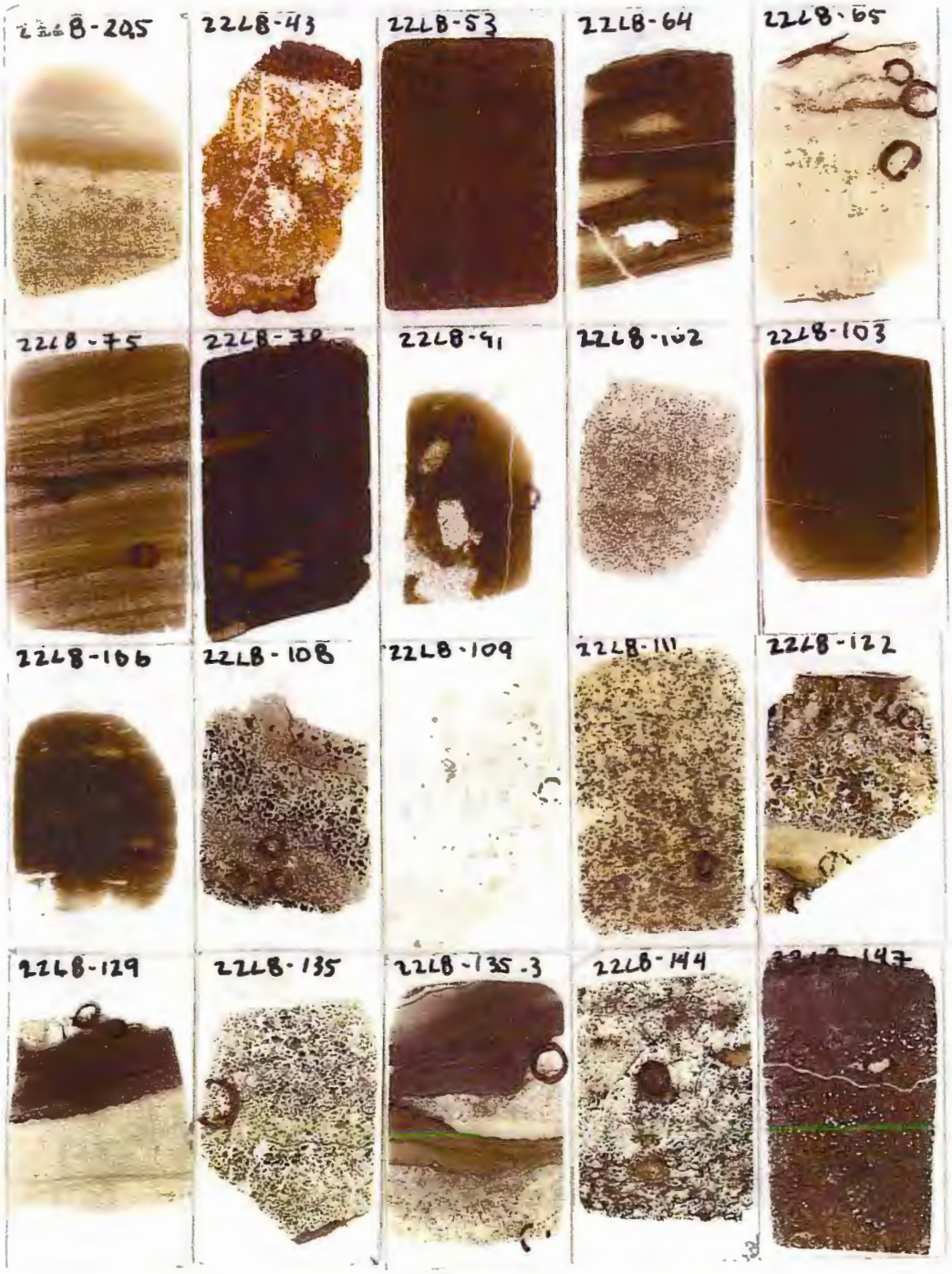
22LB-205
22LB-43
22LB-53
22LB-64
22LB-65
22LB-75
22LB-91
22LB-102
22LB-103
22LB-106
22LB-108
22LB-109
22LB-111
22LB-122
22LB-129
22LB-135
22LB-135.3
22LB-144

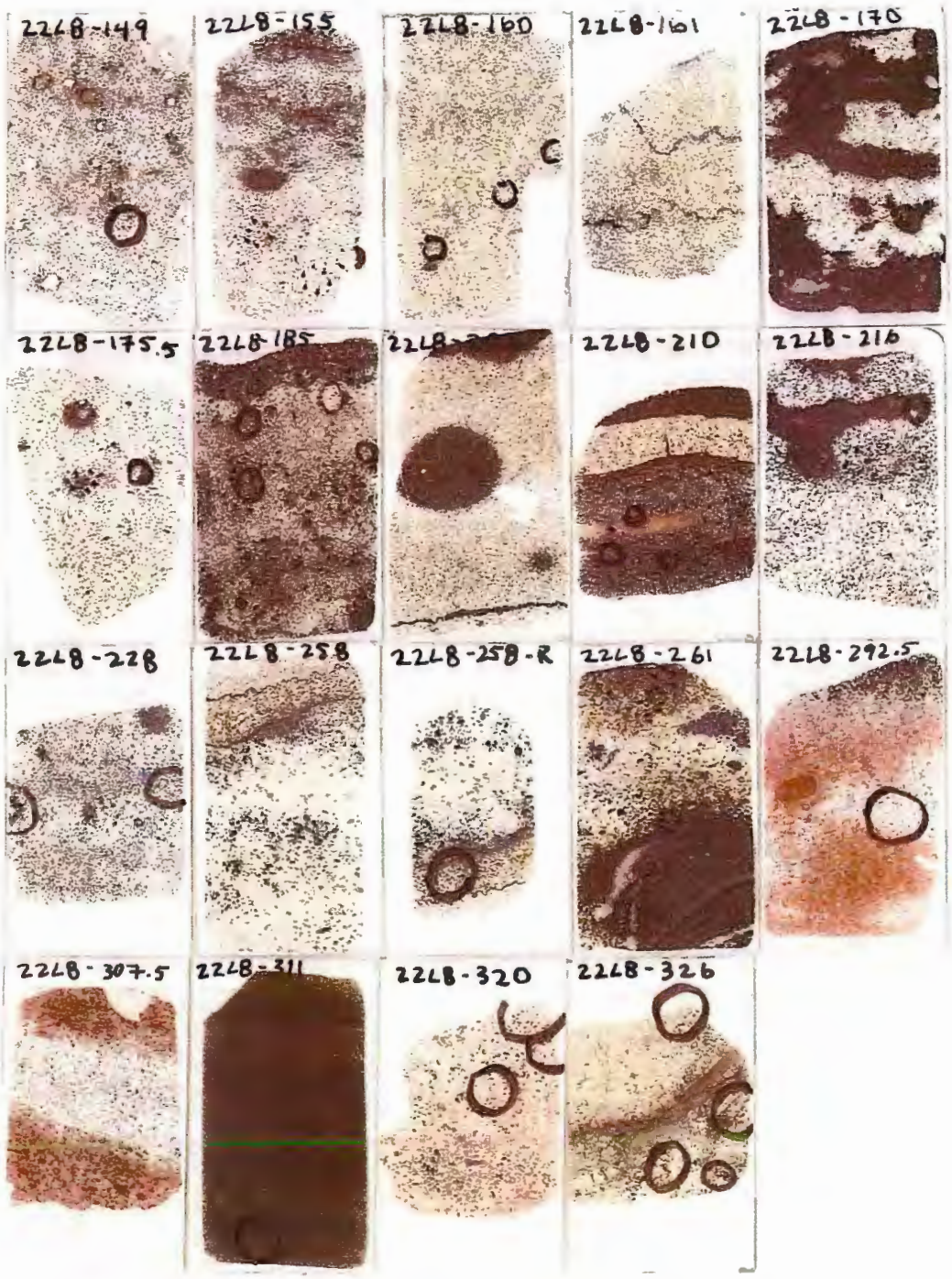
2268-149
2268-155
2268-160
2268-161
2268-170
2268-175.5
2268-185
2268-210
2268-216
2268-228
2268-258
2268-258-R
2268-261
2268-292.5
2268-307.5
2268-311
2268-320
2268-326

Appendix IV

EVTAC North Pit Fracture Measurements
July 1998

Rock Unit: Various (mostly middle upper cherty), dip of bedding varies between 8 and 15 degrees			
Measurement device: Sun Compass			
Station	**Measurement**	**Number**	**Comments**
1			no mineralization in any of the fractures
	N15W	5	
	N75W	4	prominent, 1 foot spacing, 6 feet long
	N60E	6	
	N70E	1	
2			no mineralization in any of the fractures, outcrop obscured by rocks
	N40W	4	
	N70W	1	prominent
	N30E	2	not prominent, short
	N70E	2	prominent
3			fractures spaced about 1 foot apart, weak
	N15W	1	quartz and carbonate
	N60W	3	no mineralization
	N30E	3	quartz and carbonate, minerals appear to have grown in different intervals, up to 1" wide
	N40E	3	no mineralization
4			
	N70W	1	
	N30E	4	mineralization (qtz, carb)
	N65E	2	
5			wavy bedding (stromatolite horizon?), slickensides N15W
	N60W	4	mineralization (pyrite)
	N35E	5	mineralization (qtz, carb), 1 cm wide, with quartz and carbonate slickensides on top
	N70E	4	mineralization (qtz, carb)

EVTAC North Pit Fracture Measurements
July 1998

Rock Unit: Various (mostly middle upper cherty), dip of bedding varies between 8 and 15 degrees			
Measurement device: Sun Compass			
Station	**Measurement**	**Number**	**Comments**
6			wavy bedding, no mineralization
	N30W	3	anastomosing
	N65W	2	
	N35E	2	
	N55E	2	
	N75E	3	
7			wavy bedding, bedding plane veins with slickensided top surface, slickensides N71E
	N20W	1	
	N66W	3	strong mineralization (qtz, carb)
	N25E	1	
	N80E	1	
8			wavy bedding, poorly developed joints
	N25W	1	
	N50W	4	
	N45E	1	
	N70E	1	
	N80E	3	
9			no mineralization, fractures evenly spaced from 4 to 8 inches apart
	N10W	1	
	N75W	3	is displaced when intersecting N25E
	N25E	3	
	N50E	1	
	N75E	3	

EVTAC North Pit Fracture Measurements
July 1998

Rock Unit: Various (mostly middle upper cherty), dip of bedding varies between 8 and 15 degrees			
Measurement device: Sun Compass			
Station	**Measurement**	**Number**	**Comments**
10			wavy bedding, no mineralization
	N20W	1	
	N55W	1	
	N25E	1	is displaced when intersecting N55W
	N75E	1	
11			wavy bedding, no mineralization
	N15W	2	
	N50W	1	
	N55E	1	
	N85E	3	
12			variable spacing
	N15W	1	
	N85E	2	
13			numerous anastomosing fractures, but two consistent directions
	N85W	3	
	N20W	2	

EVTAC South Pit Fracture Measurements
June 1998

Rock Unit: Lower Upper Cherty/Lower Slaty, dip of bedding variable between 9 and 21 degrees		
Measurement device: Sun Compass		
Station	**Measurement**	**Comments**
1		
	280	
	180	
2		
	230	less prominent
	240	
	320	prominent
3		
	145	prominent
	55	prominent
	100	poorly developed
4	330	
	Measurement device: GPS	
	Measurement	**Comments**
5		
	194	
	252	
	301	
6	313	prominent, long and equally spaced
7		
	186	mineralized
	206	mineralized and splays
	221	
	Additional comments: Chert nodule horizon as well as prevalent slickensides with epidote	

EVTAC Spruce Pit Fracture Measurements
June 1998

Rock Unit: Bottom of Lower Upper Cherty, dipping west		
Measurement device: Sun Compass		
Station	**Measurement**	**Comments**
1		
	290	dip vertical, fractures offset by quartz and carbonate-filled fractures
	248	least prominent, propagate shortest distance
	330	filled with quartz and carbonate
	Measurement device: GPS	
	Measurement	**Comments**
2		
	312	
	355	dip vertical
	315	
3		
	315	quartz and carbonate mineralization, creamy brown color presumably from iron carbonate
	198	offset by joints with quartz and carbonate mineralization
	214	
4		
	216	

MINNTAC East Pit Fracture Measurements
August 1999

Rock Unit: Various		
Measurement device: Sun Compass		
Station	**Measurement**	**Comments**
1		contact with upper cherty and lower slaty
	80	dip 82 north, dominant direction
	310	dip vertical
2		contact with lower slaty and lower cherty
	275	dip 81 north, dominant direction
	15	dip vertical, secondary direction
3		lower cherty, 15 to 20 ft from Pokegama quartzite
	325	dip 83 south, dominant direction
	10	dip 82 east, secondary direction
	90	dip 79 south, secondary direction
4		lower cherty, stromatolite area
	75	dip 83 northwest
	280	dip vertical

MINNTAC West Pit Fracture Measurements
August 1999

Rock Unit: Various		
Measurement device: Sun Compass		
Station	**Measurement**	**Comments**
1		lower cherty
	N80E	dip 79 N
	N80W	dip 81N, quartz/amethyst, ankerite mineralization
	N40E	dip 83 W
2		lower cherty
	N85E	dip 83 N
	N35W	dip vertical
3		upper chery/lower slaty
	90	dip 81N
	N55W	dip 86 NE
	235	dip 82 N
4		lower cherty, oxidized
	N25W	dip 80 W
	N45E	dip 87 N
	N15E	dip 81 N
5		lower slaty
	N80W	dip vertical
	N35E	dip 78 W
6		lower slaty, fissile
	N25W	dip 85 NE
	N85W	dip 81 N
	N35W	dip 86 S
	N45E	dip 78 NW

Ispat Inland Minorca Pit Fracture Measurements
June 1999

Rock Unit: Lower Cherty			
Measurement device: Sun Compass			
Station	**Measurement**	**Number**	**Comments**
1	N35E	1	No Brunton today, joints look vertical
	N45W	7	mineralized
	N10E	1	
	N25E	1	
	N20W	1	
2			joints here mutually intersect
	N5W	1	
	N55W	1	
	N45W	1	
	N20E	4	
3			wall measurements
	N10W	1	
	N40W	2	
	N55W	6	
	N20E	6	
	N40E	1	
	N50E	2	
4			striated surface
	N10E	5	
	N40W	2	
5			
	N35W	5	dip vertical
	N15E	2	
6	S55E	2	
	S35E	5	
	S30W	2	
	N80W	3	

Ispat Inland Minorca Pit Fracture Measurements
June 1999

Rock Unit: Lower Cherty			
Measurement device: Sun Compass			
Station	**Measurement**	**Number**	**Comments**
7			
	S20W	5	
	S75W	1	
	S55W	1	
	N40W	3	
8			
	N55E	3	
	N45W	5	
	N40E	3	
9			
	N25E	2	
	N70W	5	
	N50E	2	
	N10W	1	

Ispat Inland Laurentian Pit Fracture Measurements
July 1999

Rock Unit: Lower slaty			
Measurement device: Sun Compass			
Station	**Measurement**	**Number**	**Comments**
1			
	S15W	5	
	S25W	3	
	S20W	2	
	S80E	2	
	S65E	2	
2			
	N20E	2	
	S50E	2	
	N45W	2	
	S10E	2	
3			
	N55W	3	dip vertical
	N80E	4	dip vertical
4			
	S75E	4	
	N60E	3	
	S70E	1	
5			
	N10E	1	
	N70W	2	
	N50W	3	
	N70E	3	
	S70W	1	

Appendix V

Jirsa/Boerboom Late Archean Fracture Measurements

Calculation Method - Frequency

Class Interval - 10 Degrees

Data Type - Bidirectional

Population - 257

Maximum Percentage - 8

R-mag - 0.08

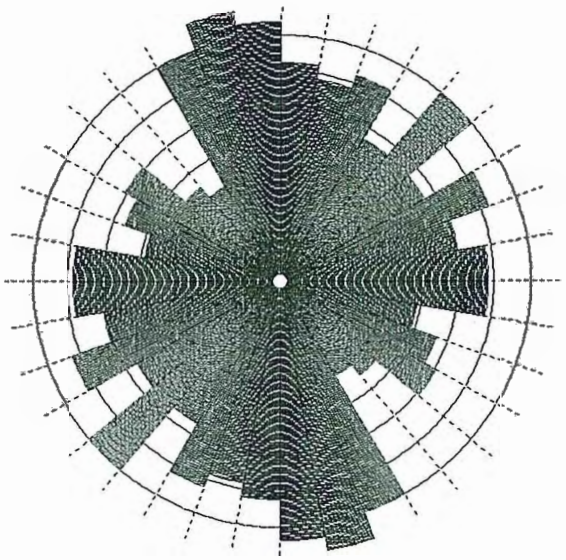

Jirsa/Boerboom Biwabik Iron Formation and Pokegama Quartzite Fracture Measurements

Calculation Method - Frequency

Class Interval - 10 Degrees

Data Type - Bidirectional

Population - 8

Maximum Percentage - 12.5 Percent

R-mag - 0.15

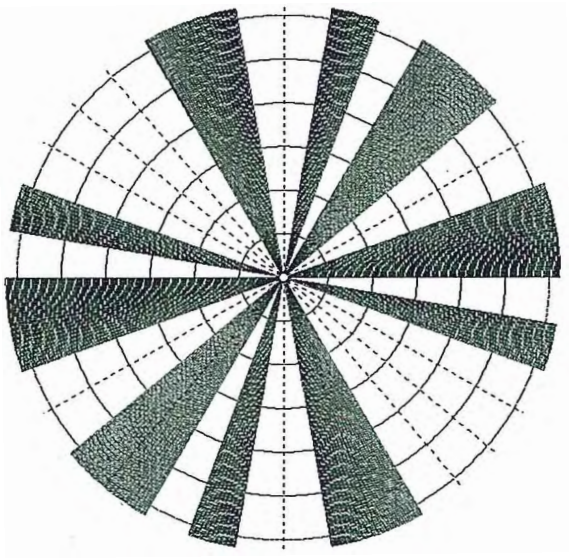

Combined Pit Fracture Measurements

Calculation Method - Frequency

Class Interval - 10 Degrees

Data Type - Bidirectional

Population - 299

Maximum Percentage -12.7 Percent

R-mag - 0.03

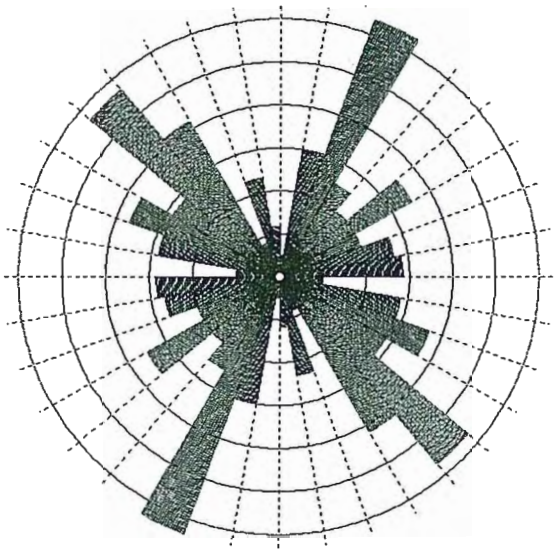

EVTAC North Pit Fracture Measurements

Calculation Method - Frequency

Class Interval - 10 Degrees

Data Type - Bidirectional

Population - 111

Maximum Percentage - 11.7 Percent

R-mag - 0.16

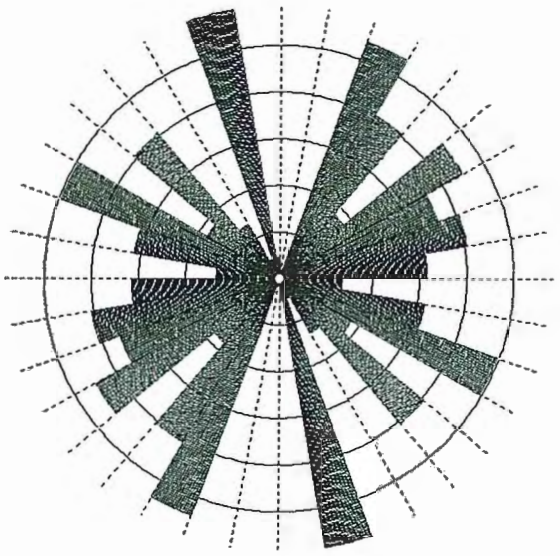

EVTAC South Pit Fracture Measurements

Calculation Method - Frequency

Class Interval - 10 Degrees

Data Type - Bidirectional

Population - 16

Maximum Percentage - 12.5 Percent

R-mag - 0.04

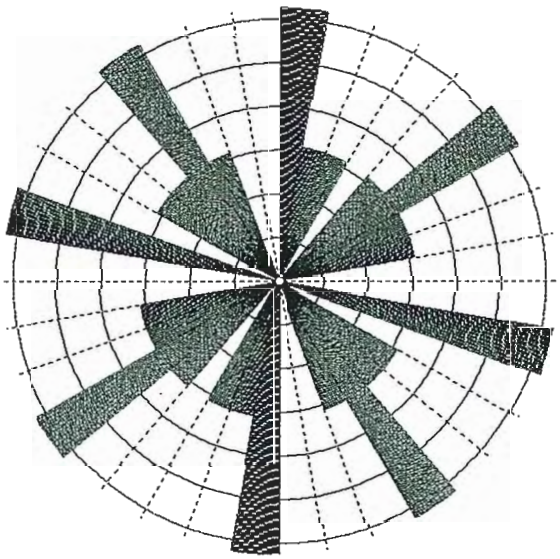

EVTAC Spruce Pit Fracture Measurements

Calculation Method - Frequency

Class Interval - 10 Degrees

Data Type - Bidirectional

Population - 10

Maximum Percentage - 30 Percent

R-mag - 0.21

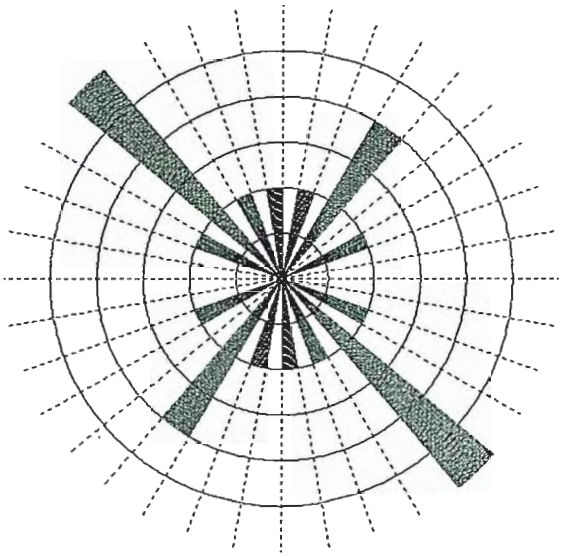

MINNTAC East Pit Fracture Measurements

Calculation Method - Frequency

Class Interval - 10 Degrees

Data Type - Bidirectional

Population - 9

Maximum Percentage - 22.2 Percent

R-mag - 0.31

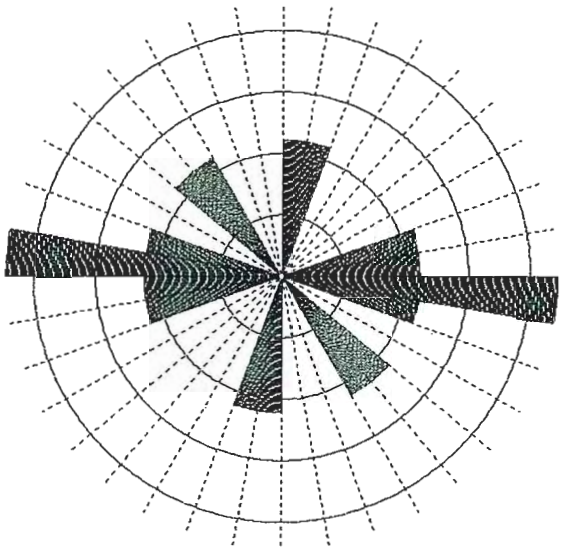

MINNTAC West Pit Fracture Measurements

Calculation Method - Frequency

Class Interval - 10 Degrees

Data Type - Bidirectional

Population - 17

Maximum Percentage - 17.6 Percent

R-mag - 0.19

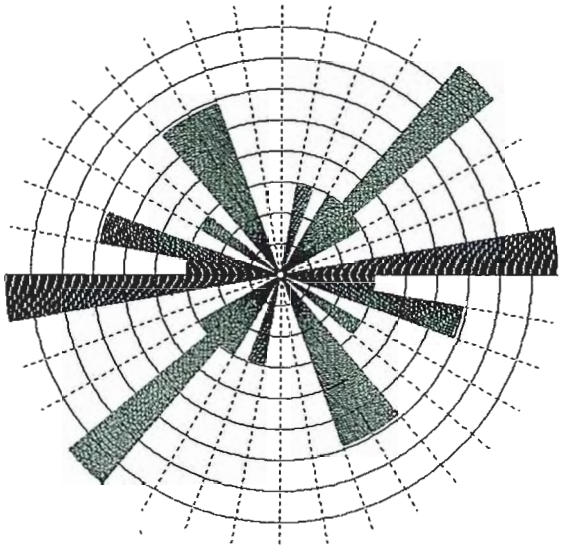

Ispat Inland Minorca Pit Fracture Measurements

Calculation Method - Frequency

Class Interval - 10 Degrees

Data Type - Bidirectional

Population - 93

Maximum Percentage - 19.4 Percent

R-mag - 0.23

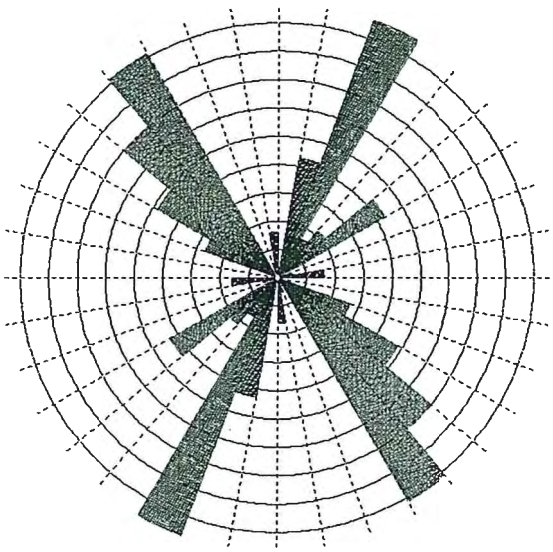

Ispat Inland Laurentian Pit Fracture Measurements

Calculation Method - Frequency

Class Interval - 10 Degrees

Data Type - Bidirectional

Population - 43

Maximum Percentage - 16.3 Percent

R-mag - 0.11

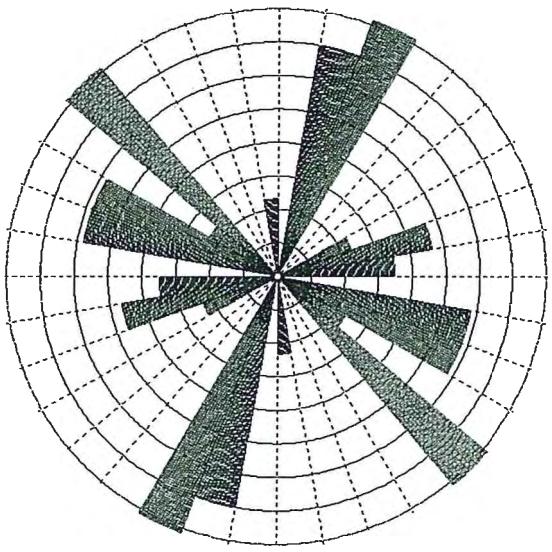

REFERENCES

Austin, G., 1972, Cretaceous Rocks: In Sims P., and G. Morey (ed.), Geology of Minnesota: A Centennial Volume, Minnesota Geological Survey, p. 509-512.

Boese, D., 1975, John C. Greenway and the Opening of the Western Mesabi: Itasca Community College Foundation, Grand Rapids, 222 p.

Boggs, S., Jr., 1995, Principles of Sedimentology and Stratigraphy: Second edition, Simon and Schuster Company, New Jersey, 774 p.

Cannon, W., 1998, Understanding the middle Proterozoic history of the Lake Superior region: what's new? what's next? Institute on Lake Superior Geology Program and Abstracts, v. 44, Minneapolis, May 6-10, p.19-21.

Clark, G., 1987, Principles of Rock Fragmentation, Wiley and Sons, New York, 610 p.

Condie, K., D. Des Marais, and D. Abbot, 2000, Geologic evidence for a mantle superplume event at 1.9 Ga: Geoscience Geophysics Geosystems (online journal), v. 1, paper number 2000GC000095.

Crowell, B., 1927, The Iron Ores of Lake Superior, Penton Press, Cleveland, 365 p.

Davis, J., 1986, Statistics and Data Analysis in Geology: Second edition, Wiley and Sons, New York, 646 p.

Evans, A., 1993, Ore Geology and Industrial Minerals: An Introduction: Third edition, Blackwell Science, London, 389 p.

Fralick, P., Kissen, S., and Davis, D.W., 2002, The age of the Gunflint Formation, Ontario, Canada: single zircon U-Pb age determination from reworked volcanic ash: Canadian Journal of Earth Science, v. 39, p. 1085 – 1091.

French, B., 1973, Mineral assemblages in diagenetic and low-grade metamorphic iron-formation: Economic Geology, v. 68, p. 1063-1074.

Gaines R, H. C. Skinner, E. Ford, B. Mason, and A. Rosenzwerg (eds), 1997, Dana's New Mineralogy: The System of Mineralogy of James Dwight Dana and Edward Salisbury Dana: Eighth edition, John Wiley and Sons, New York, 1819 p.

Gole, M. and C. Klein, 1981, Banded iron-formations through much of Precambrian time: Journal of Geology, v. 89, p. 169-183.

Goodwin, A., 1975, Facies relations in the Gunflint iron-formation: In Lepp, H. (ed.)

Geochemistry of Iron: Benchmark Papers in Geology, v. 18, Dowden, Hutchinson and Ross, Inc., Stroudsburg, p. 286-290.

Govett, G., 1966, Origin of banded iron formations: In Lepp, H. (ed.) Geochemistry of Iron: Benchmark Papers in Geology, v. 18. Dowden, Hutchinson and Ross, Inc., Stroudsburg. p. 361-380.

Gribble, C. and A. Hall, 1992, Optical Mineralogy: Principles and Practice, UCL Press, London, 303 p.

Gross, G. 1973, The depositional environment of principal types of Precambrian iron-formation: In Genesis of Precambrian Iron and Manganese Deposits. Proceedings of the Kiev Symposium, 10-25 August 1970, UNESCO, Paris, p. 15-21.

Gruner, J., 1944, The composition and structure of minnesotaite: The American Mineralogist, v. 29, p. 363-372.

Gruner, J., 1946, The Mineralogy and Geology of the Taconites and Iron Ores of the Mesabi Range, Minnesota, IRRB, St. Paul, 127 p.

Hatcher, R., 1995, Structural Geology: Principles, Concepts, and Problems: Second edition, Prentice Hall, Englewood Cliffs, 525 p.

Hoffman, P., 1987, Early Proterozoic foredeeps, foredeep magmatism and Superior-type iron-formations of the Canadian Shield: American Geophysical Union Geodynamics Series, v. 17, p. 85-948.

Holway, W. 1956, Auburn Mine field trip guide – stop no. 12. Oliver Mining Division, US Steel Corporation, Virginia, Minnesota: In, Schwartz, G. (ed.), Guidebook for field trips: field trip number 1: Precambrian of Northeastern Minnesota, Geological Society of America, Minneapolis meeting, p. 160-167.

Isley, A., 1995, Hydrothermal plumes and the delivery of iron to banded iron formation: Journal of Geology, v. 103, p. 169-185.

James, H., 1954, Sedimentary facies of iron-formation: Economic Geology, v. 49, p. 235-293.

James, H., 1966, Chemistry of the iron-rich sedimentary rocks: In Lepp, H. (ed.) Geochemistry of Iron: Benchmark Papers in Geology, v. 18. Dowden, Hutchinson and Ross, Inc., Stroudsburg, p. 41-52.

Jongewaard, P., 1998, personal communication. Geologist, Peter Jongewaard, EVTAC, Eveleth, Minnesota.

Juneau, P., 1979. Origin and petrology of iron silicate-rich bodies in the Biwabik Iron Formation, Minnesota: University of Minnesota M.S. Thesis, 209 p.

Klein, C. 1983. Diagenesis and metamorphism of Precambrian banded iron formations: In Trendall, A., and R. Morris, (eds.) Iron-Formation: Facts and Problems. Developments in Precambrian Geology 6, Elsevier, New York, p 417-471.

Klein, C., and C. Hurlbut, 1985, Manual of Mineralogy, Wiley and Sons, New York, 681 p.

LaBerge, G., 1964, Development of magnetite in iron-formations of the Lake Superior region. Economic Geology, v. 59, p. 1313-1342.

Lepp, H., (ed), 1975, Introduction: In Lepp, H. (ed.) Geochemistry of Iron: Benchmark Papers in Geology, v. 18. Dowden, Hutchinson and Ross, Inc., Stroudsburg, p. 1-11.

Lepp, H., and S.S. Goldich. 1964. Origin of Precambrian iron formations. In Lepp, H. (ed.) Geochemistry of Iron: Benchmark Papers in Geology, v. 18. Dowden, Hutchinson and Ross, Inc., Stroudsburg, p 252-264.

Morey, G. B., 1970, Mesabi, Gunflint and Cuyuna ranges, Minnesota: In Genesis of Precambrian Iron and Manganese Deposits. Proceedings of the Kiev Symposium, 10-25 August 1970. UNESCO, Paris, 1973, p. 193-208.

Morey, G. B., 1972, Mesabi Range: In Sims P., and G. Morey (ed.), Geology of Minnesota: A Centennial Volume, Minnesota Geological Survey, p. 204-217.

Morey, G. B., 1983, Animike basin, Lake Superior region, U.S.A., In Trendall, A., and Morris, R., eds, in Iron-formation: Facts and problems, Amsterdam, Elsevier, p. 13-67.

Morey, G. B., 1992, Chemical composition of the Eastern Biwabik iron-formation (early Proterozoic), Mesabi Range, Minnesota: Economic Geology, v. 87, p. 1649-1658.

Morey, G. B., 1999, High-grade iron ore deposits of the Mesabi Range, Minnesota—product of a continental-scale Proterozoic ground-water flow system: Economic Geology, v. 94, p. 133-142.

Morey, G. B., and R. Ojakangas, 1970, Sedimentology of the Middle Precambrian Thomson Formation, east-central Minnesota: Minnesota Geological Survey Report of Investigation 13, 32 p.

Morey, G. B., and D. Southwick, 1995, Allostratigraphic relationships of Early Proterozoic iron-formations in the Lake Superior Region: Economic Geology, v. 90, p. 1983-1993.

Ojakangas, G., 1996, Cyclic tidal laminations in the early Proterozoic Pokegama formation: digital image analysis and computer modeling (abs.); 42nd Institute on Lake Superior Geology Proceedings v. 42, Cable, WI, p. 44-45.

Ojakangas, R., 1972, Archean volcanogenic graywackes of the Vermilion district, northeastern Minnesota: Geologic Society of America Bulletin, v. 83, p. 429-442.

Ojakangas, R., 1983, Tidal deposits in the early Proterozoic basin of the Lake Superior region – The Palms and the Pokegama formations: evidence for subtidal-shelf deposition of Superior-type banded iron-formation: In Medaris, L., Jr., (ed.) Early Proterozoic Geology of the Great Lakes Region: Geological Society of America Memoir 160, p. 49-66.

Ojakangas, R., 1994. Sedimentology and provenance of the Early Proterozoic Michigamme Formation and Goodrich Quartzite, northern Michigan-Regional stratigraphic implications and suggested correlations: U.S. Geological Survey Bulletin 1904-R, 31 p.

Ojakangas, R., 1996. Tidalites of Early Proterozoic age in the western Lake Superior Region: Minnesota, Wisconsin, and Michigan (abs.): Institute of Lake Superior Geology Proceedings, v. 42, p. 46-47.

Ojakangas, R., 1999, personal communication. Geology professor, Dr. Richard Ojakangas, University of Minnesota, Duluth.

Patterson, C., 1998, Models for interpreting the Quaternary history of Lake Superior Region (abs.), in Institute of Lake Superior Geology Proceedings v. 44, p. 33.

Perry, E. Jr., and F. Tan, 1973, Significance of carbon isotope variations in carbonates from the Biwabik iron-formation, Minnesota. In Lepp, H. (ed.) Geochemistry of Iron: Benchmark Papers in Geology, v. 18. Dowden, Hutchinson and Ross, Inc., Stroudsburg, p. 398-404.

Pollard, D., and A. Aydin, 1988, Progress in understanding jointing over the past century. Geological Society of America Bulletin v. 100, p. 1181-1204.

Rankama, K., 1955, Geologic evidence of chemical composition of the Precambrian atmosphere: Geologic Society of America Special Paper 62, p. 651–664.

Simonson, B., 1987, Early silica cementation and subsequent diagenesis in arenites from four early Proterozoic iron-formations of North America: Journal of Sedimentary Petrology, v. 57, no. 3, p. 494-511.

Simonson, B., and S. Hassler, 1996, Was the deposition of large Precambrian iron-formations linked to major marine transgressions? The Journal of Geology, v. 104, p. 665-676.

Sims, P., and G. Morey, 1972, Resume of Geology of Minnesota: In Sims P., and G. Morey (ed.), Geology of Minnesota: A Centennial Volume, Minnesota Geological Survey, p. 3-17.

Southwick and Morey, 1991, Tectonic imbrication and foredeep development in the Penokean orogen, east-central Minnesota-an interpretation based on regional geophysics and the results of test drilling: U.S. Geological Survey Bulletin 1904-C, 17 p.

Spurr, J., 1894, The Mesabi Iron Bearing Rocks: University of Minnesota Press, Minneapolis, 268 pages.

Walter, M., 1976, Stromatolites: Developments in Sedimentology 20, Elsevier, New York, 790 pages.

White, D., 1954, The stratigraphy and structure of the Mesabi Range, Minnesota: Minnesota Geological Survey Bulletin 38, University of Minnesota Press, Minneapolis, 89 pages.

Winter, B., and L. Knauth, 1992, Stable isotope geochemistry of cherts and carbonates from the 2.0 Ga Gunflint Iron-Formation: implications for the depositional setting, and the effects of diagenesis and metamorphism: Precambrian Research, v. 59, 283-313.

Wolff, J., 1917, Recent geologic developments on the Mesabi Range, Minnesota: American Institute of Mining and Metallurgic Engineers Trans., v. 56, p. 142-169.